ACS OMEGA

http://pubs.acs.org/journal/acsodf

Article

Geochemical Characteristics of Three Oil Families and Their Possible Source Rocks in the Sub-Sag A of Weixinan Depression, Beibuwan Basin, Offshore South China Sea

Xiaoxiao Ma, Lin Wei,* Dujie Hou,* Changgui Xu, Yong Man, Wenlong Li, and Piao Wu

Cite This: *ACS Omega* 2022, 7, 24795−24811

Read Online

ACCESS | Metrics & More | Article Recommendations

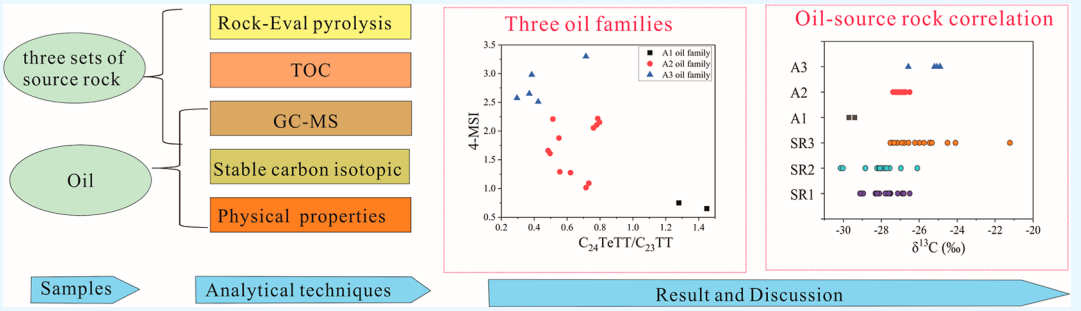

ABSTRACT: Three oil families from the sub-sag A of the Weixinan Depression are identified by integrated analysis of physical properties, stable carbon isotopes, and gas chromatography−mass spectrometry (GC−MS). Their similarities and differences in relative thermal maturities, depositional environments, and biological sources of organic matter (OM) are investigated. A possible oil−source correlation of this area is established. Group A1 oils, defined as low-maturity oils, are characterized by high density and high viscosity. They contain more terrigenous OM deposited in a freshwater environment with unstratified water columns reflected by a relatively high terrestrial/aquatic ratio and Pr/Ph values, low abundance of C_{30} 4-methlysteranes, and low $\delta^{13}C$ values. They are derived from the upper hydrocarbon supply combination. Group A2 oils are characterized by moderate density and viscosity and medium stable carbon isotope values. This group of oils has lower terrestrial/aquatic ratios and Pr/Ph values and a medium concentration of C_{30} 4-methlysteranes and $\delta^{13}C$ values, suggesting that the oils are derived from the shales which have more contribution from the algal input and are formed in a weakly oxidizing environment. They are a mixture generated from the source rocks in the middle and lower hydrocarbon supply combination. Groups A3 oils, defined as light oils, have low density and viscosity. The geochemical data of the A3 oils, including a less-negative stable carbon isotope, high abundance of C_{30} 4-methylsteranes, low Pr/Ph values, and highest Ts/(Ts + Tm) ratios (Ts represents C_{27} 18α(H)-22,29,30-trisnorneohopane and Tm represents C_{27} 17α(H)-22,29,30-trisnorhopane), suggest that they are generated from the source rocks deposited in a subanoxic environment with the large input of dinoflagellates. The A3 oils are generated from the shales from the lower hydrocarbon supply combination. The oil−source correlation results can be further supported by the distribution of faults and structural ridge as the migration channel of petroleum developed around the sub-sag A.

1. INTRODUCTION

The Beibuwan Basin is a fault-depression superimposed basin dominated by Cenozoic sedimentation in the northern continental shelf sea of the South China Sea. It has an area of 3.98 × 10^4 km^2.[1] The Weixinan Depression (Figure 1a), located in the north part of the Beibuwan (BBW) Basin, is one of the petroliferous depressions. Three faults controlled the development of the Weixinan Depression. The Weixinan fault controls the deposition of Changliu Formation. In Eocene, with the weakening of Weixinan fault activity, no. 1 fault became more active and controlled the sediments of the Liushagang Formation. In Oligocene, as the activity of no. 1 fault weakened, the activity of no. 2 fault gradually increased and developed into a main fault controlling the deposition of the Weizhou Formation.[2] According to the distribution of depocenter of Paleogene Liushagang Formation, the depression was further divided into sub-sags A, B, and C.[3] Due to the differences in later structural evolution and burial history, these

Received: May 6, 2022
Accepted: June 22, 2022
Published: July 8, 2022

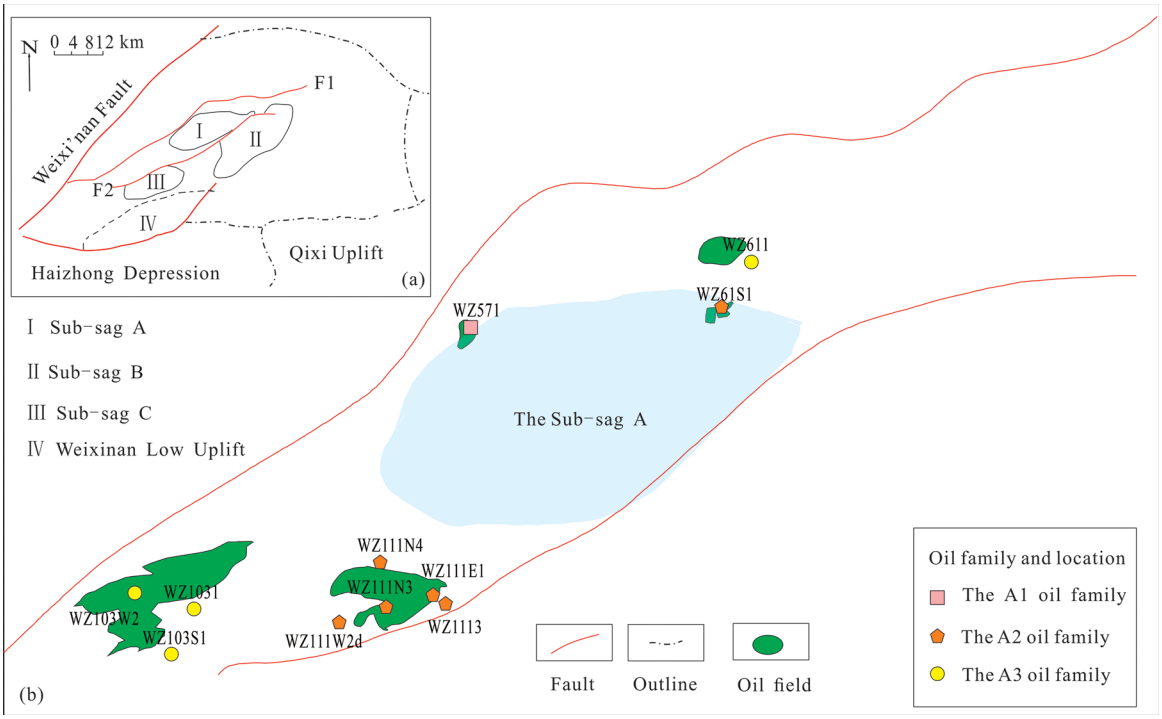

Figure 1. Geological maps showing the tectonic distribution units of the Weixinan sag (a) and the distribution of the three major oil families in the sub-sag A (b).

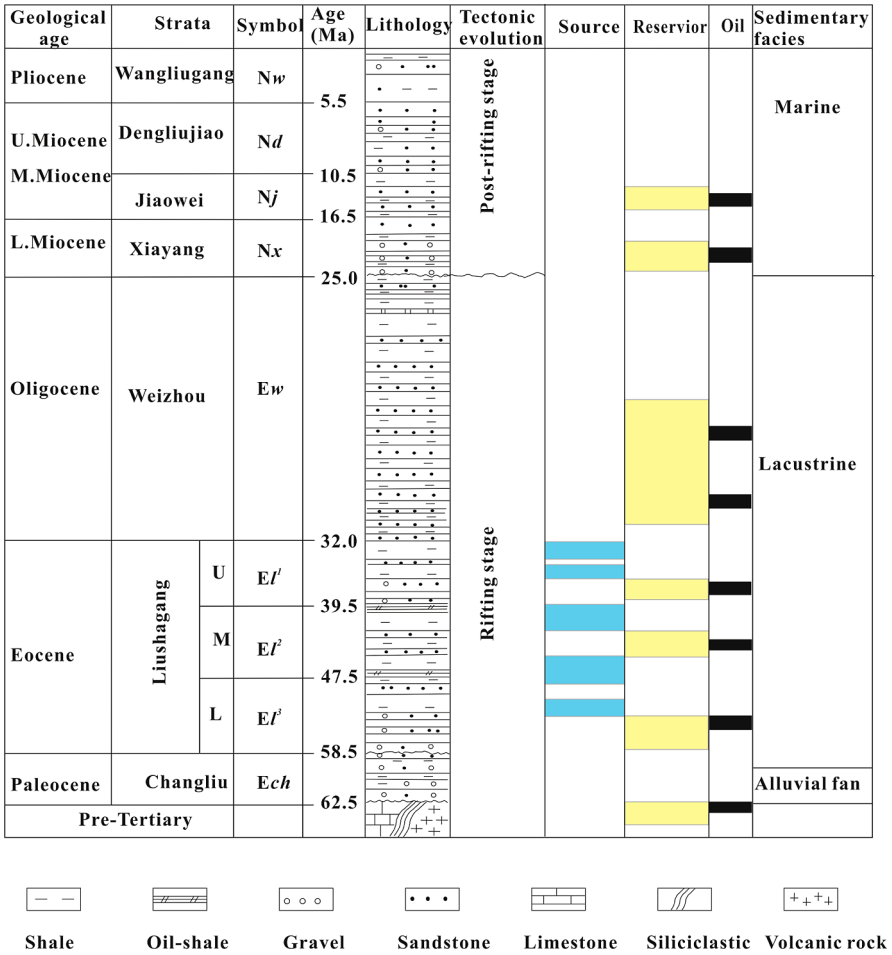

Figure 2. Generalized stratigraphic column of the Weixinan sag.

https://doi.org/10.1021/acsomega.2c02826
ACS Omega 2022, 7, 24795−24811

Table 1. Physical Properties of Three Oil Families in the Sub-Sag A of the Weixinan Sag[a]

oil field	form.	density (g/mL, 20 °C)	viscosity (mPa s)	wax (%)	sulfur (%)	oil family
WZ103	El^3	0.83−0.81/0.85	4.60−9.71/5.88	28.20−38.50/25.15	0.01−0.20/0.08	A3
WZ103W	El^3	0.76−0.84/0.82	0.64−12.13/5.57	1.63−24.39/18.22	0.05−0.11/0.09	A3
WZ111	E*j*	0.92	98	8.75	0.27	A2
WZ111	El^3	0.81−0.89/0.85	2.64−84.46/27.62	12.24−31.1/22.60	0.06−0.31/0.16	A3
WZ111	E*ch*	0.83−0.84/0.83	4.46−6.53/5.29	11.01−17.33/14.56	0.08−0.09/0.09	A3
WZ111E	E*j*	0.92	236.39	1.19	0.31	A2
WZ111N	El^1	0.86−0.87/0.87	21.22−67.47/43.87	14.33−18.42/16.11	0.22−0.29/0.25	A2
WZ111W	E*w*	0.865−0.87/0.87	19.26−22.79/21.12	12.30−12.70/12.50	0.20−0.20/0.20	A2
WZS7	El^1	0.90−0.92/0.91	70.77−119.4/95.09	17.25−17.43/17.34	0.40−0.50/0.45	A1
WZ61S	El^1	0.85−0.86/0.86	12.11−18.05/14.91	15.13−20.42/18.52	0.16−0.20/0.18	A2

[a]Note: each cell consists of two parts, above the horizontal line is the range (minimum to maximum) and below is the average.

Table 2. Bulk Carbon Isotopic Composition of the A1, A2, and A3 Oil Families from the Sub-Sag A of the Weixinan Sag[a]

						$\delta^{13}C_{PDB}$ (‰)				
no.	field	well	depth (m)	form.	oil family	whole Oil	saturate	aromatic	NSO	asphaltene
S01	WZS7	WZS71	2820.9	E*w*	A1	−29.40	−30.60	−28.70	n.d.	n.d.
S02	WZS7	WZS71	2831.9	El^1	A1	−29.70	−31.13	−27.43	−27.80	−28.43
S03	WZ111	WZ1113	995.5	E*j*	A2	−26.79	−27.15	−25.02	−26.19	−26.67
S04	WZ111E	WZ111E1	986	E*j*	A2	−26.50	−27.40	−26.10	−25.96	−26.50
S05	WZ111E	WZ111E1	991	E*j*	A2	−26.71	−27.13	−24.74	−26.14	−26.38
S06	WZ111E	WZ111E1	995	E*j*	A2	−26.50	−27.10	−25.80	−25.90	−26.40
S07	WZ111N	WZ111N3	2097.25	El^1	A2	−27.24	−28.15	−25.72	−26.35	−26.62
S08	WZ111N	WZ111N4	2088.25	El^1	A2	−27.23	−27.69	−25.31	−26.39	−26.71
S09	WZ111W	WZ111W2d	1582.04	E*w*	A2	−27.22	−28.16	−26.50	−26.64	−26.98
S10	WZ111W	WZ111W2d	1551.01	E*w*	A2	−27.38	−28.12	−26.84	−27.06	−27.41
S11	WZ61S	WZ61S1	1808	E*w*	A2	−27.20	−27.70	−26.40	n.d.	n.d.
S12	WZ61S	WZ61S1	1812.1	E*w*	A2	−27.10	−27.60	−26.50	n.d.	n.d.
S13	WZ61S	WZ61S1	1972.8	El^1	A2	−26.90	−27.40	−26.30	n.d.	n.d.
S14	WZ61S	WZ61S1	1991.3	El^1	A2	−27.00	−27.50	−26.20	n.d.	n.d.
S15	WZ103	WZ1031	2033	El^3	A3	−25.20	−25.40	−23.27	−24.32	−25.54
S16	WZ103S	WZ103S1	2286.5	El^3	A3	−25.07	−25.22	−23.80	−24.22	−24.94
S17	WZ103W	WZ103W2	2104.5	El^3	A3	−24.90	−25.20	−24.40	−24.20	−24.90
S18	WZ111	WZ1112	2856.1	E*ch*	A3	−26.57	−26.91	−24.53	−24.93	−25.44
S19	WZ61	WZ611	1967	El^3	A3	−24.91	−25.00	−23.42	−24.23	−25.01

[a](Note: NSO = nitrogen-, sulfur-, and oxygen-bearing compounds).

three subsags are differentiated in hydrocarbon generation evolution.

Over the past 30 years, a group of commercial oil-bearing structures and oil fields have been discovered in the Weixinan Depression, especially in sub-sag B (Figure 1a). However, according to previous exploration results, sub-sag A has a certain area larger than sub-sag B, and the shales from sub-sag A have great hydrocarbon potential as well, but only a small amount of oil has been discovered. Therefore, the exploration and research on the sub-sag A become a focus. Previous studies on crude oils in the Weixinan Depression have focussed on oil classification, oil−source correlation, and hydrocarbon accumulation conditions on the scale of the whole basin or particular area (e.g., sub-sag C, the southeast slope and WZ12 oil field). For example, Huang et al.[4] and Fan et al.[1] recognized three different oil groups generated from the Liushagang Formation. In comparison, Fan et al.[1] believed that the first type of oils was derived from the bottom of the first member of the Liushagang Formation (El^1) and the top of the second member of the Liushagang Formation (El^2), the last two types of oils were generated from the bottom of the El^2 formation and the top of the third member of the Liushagang Formation (El^3) in the Weixinan Depression. The studies on the WZ12 oil field by Jin[5] and Wang et al.[6] revealed that these oils were from the El^2 and El^3 source rocks. As outlined above, these previous organic geochemical studies on the crude oils from the Weixinan Depression were conducted on the samples mostly from sub-sag B, such as the WZ12 oil field.[6] Nevertheless, the geochemical characteristics and possible source rocks of crude oils from the sub-sag A have not yet been studied in detail. Compared to the sub-sag B, the petroleum system of sub-sag A remains unclear.

The aims of this work are to investigate the basic geochemical characteristics of the oils, define oil families, and to make an oil−source correlation in order to achieve a better understanding of the petroleum system in sub-sag A.

2. GEOLOGICAL BACKGROUND

The Beibuwan Basin, located in the northern continental shelf area of the South China Sea, is a Mesozoic−Cenozoic extensional basin with an area of 3.98×10^4 km^2. The Weixinan Depression, which is located in the northern BBW Basin, has an area of about 3454 km^2. It is adjacent to the Weixinan fault in the north and the no. 3 fault in the south.

The structural evolution of the Weixinan sag was characterized by two stages separated by unconformities

https://doi.org/10.1021/acsomega.2c02826
ACS Omega 2022, 7, 24795−24811

(Figure 2): Eocene−Oligocene extensional phase marked by fault bounded and rifted strata and the Miocene-recent passive margin phase.[4,7] The Eocene−Oligocene rifting stage began in the Chuangliu Formation (E*ch*) characterized by a coarse-grained conglomerate with interbedded sandstone and shale. The Liushagang Formation (E*l*) is subdivided into upper (El^1), middle (El^2), and lower (El^3) sections on the basis of their lithology and fossil assemblages. It widely consists of a combination of dark shale, which is the effective source rock in the Weixinan Depression. The Weizhou Formation (E*w*) is dominated by sandstone and also contains dark mudstone. The postrift marine sediments of the Miocene to Pleistocene consist mainly of sandstone interbedded with mudstones (Figure 2).

In the Weixinan Depression, BBW Basin, hydrocarbon reservoirs have been discovered within the El^3, El^1, E*w*, E*j*, and E*x* sand stones (Figure 2). Available geological data have suggested that the oil fields are sourced from E*l* rocks, which include from bottom to top, El^3, El^2, and El^1 formations.[4,8,9] Among them, two layers of organic-rich shale (oil shale) were deposited at the top and bottom of the seconder member of Liushagang Formation (El^2). Fu and Liu[10] and Fu[11] suggested that although it is considered that the main source rocks in the BBW Basin are lacustrine shales of the El^2 formation, these shales vary in the quality.

3. MATERIALS AND METHODS

A series of 19 crude oils from the sub-sag A in the Weixinan Depression, northern Beibuwan Basin were chosen in this work. The well locations are shown in Figure 1b, and the detailed information on these samples is shown in Table 1. A total of 136 source rocks were chosen for Rock-Eval pyrolysis and total organic carbon (TOC) analyses, and 20 source rocks were chosen for gas chromatography−mass spectrometric (GC−MS) analyses (Tables 1−5).

3.1. Rock-Eval Pyrolysis and Total Organic Carbon Analyses. The TOC was measured based on the standard process (SY/T 5116-1997) using LECO CS-230. The pyrolysis analysis was conducted on the Rock-Eval instrument,[12] and the parameters including the free hydrocarbon (S_1), potential hydrocarbon (S_2), and maximum temperature of hydrocarbon generation (T_{max}) were obtained.

3.2. Gas Chromatography−Mass Spectrometry Analyses. About 20−30 mg of each crude oil was separated into saturated hydrocarbons and aromatic hydrocarbons on a short activated neutral alumina column using *n*-hexane and *n*-hexane/dichloromethane (1:2, v/v). The surficial contamination of the cutting samples was removed through rinsing with deionized water and alcohol before powdering into 200 mesh. Extractable organic matter was extracted from the ground samples in chloroform using a Soxhlet apparatus for 72 h. Then, the method of separation of saturated hydrocarbons is the same as that of oils. The saturated hydrocarbons were analyzed on an Agilent 7890 gas chromatograph interfaced to an Agilent 5975c mass spectrometer (70 eV ionization energy) as described by Ding et al.[13] The oven temperature was initially held at 50 °C (held for 1 min), then heated up to 120 °C at a rate of 20 °C/min, programmed from 120 to 250 °C at 4 °C/min, and finally to 310 °C (held at 310 °C for 30 min) at 3° C/min. The selective ion mode and full scan were used for the data acquisition.

3.3. Stable Carbon Isotope Analyses of Fractions. The stable carbon isotope ($\delta^{13}C$) analysis of whole oils and source rock kerogens was carried out using a Finnigan MAT-251 mass spectrometer as describe by Cai et al.[14] Stable carbon isotope measurements were made on the aliphatic and the aromatic hydrocarbon fractions of oil samples as well. The $^{13}C/^{12}C$ isotope ratio of the CO_2 generated from a sample was compared with the corresponding ratio of a reference, calibrated against the PDB standard. The reproducibility of the total analytical procedure is in the range of 0.1−0.2‰.

4. RESULTS AND DISCUSSION

4.1. Geochemical Characteristics of Oils. Based on the bulk composition, the saturated hydrocarbon biomarker distributions, and stable carbon isotopic data of the studied oils from the sub-sag A, they can be divided into three families: the A1 oil family, the A2 oil family, and the A3 oil family (Table 1). The distribution of three types of oils is shown in Figure 1b. The A1 oil family is mainly from the WZ57 oil field, and the A2 oil family is mainly from WZ111, WZ111E, WZ111N, WZ1111W, and WZ61S oil fields. The A3 oil family is distributed in the El^3 formation of WZ103, WZ103W, WZ103S, and WZ61 oil fields. The basic geochemical characteristics of the oil families and comparison of their similarities and differences in biomarker were conducted in this study.

4.1.1. Physical Properties. The physical properties of crude oil show a huge difference among these three oil families (Figure 3a). Density of crude oils is widely used to classify the light crude oil (0.80−0.87 g/mL), medium crude oil (0.87−0.89 g/mL), and heavy crude oil (0.89−0.93 g/mL).[15] Density of oils from the El^2, El^3 and E*ch* formations typically ranges from 0.76 to 0.89 g/mL (average = 0.85 g/mL; Table 1), classifying the oil as the light crude oil. The medium and heavy oils are observed in the E*w*, E*j*, and El^1 formations in the WZ111W, WZ111E, and WZ57 reservoirs, respectively. The A1 oil family is characterized by a high density (0.90−0.92 g/mL; average = 0.91 g/mL; Table 1 and Figure 3a), a high viscosity (70.77−119.4 mPa s; average = 95.09 mPa s), a medium wax content (17.25−17.43%; average = 17.34%), and a high sulfur content (0.40−0.50%; average = 0.45%). Compared with the A1 oil family, the oils from the A2 oil family, except for oils from WZ111E1 and WZ1113, have a lighter density (0.85−0.87 g/mL; average = 0.86 g/mL), a lower viscosity (12.11−67.47 mPa s; average = 28.18 mPa s), a medium wax content (12.30−20.42%; average = 16.26%; Table1), and a lower sulfur content (0.16−0.29%; average = 0.22%; Table 1). The A3 oil family is characterized by a low density (0.82−0.87 g/mL; average = 0.84 g/mL; Table 1), a low viscosity (4.3−32.8 mPa s; average = 7.97 mPa s; Table 1), a slightly higher wax content (13.5−29.28%; average = 21.87%; Table1), and the lowest sulfur content (0.01−0.22%; average = 0.10%; Table 1). In general, the physical properties are affected by thermal maturity, biological sources of organic matter (OM), and secondary effects.[15] Heavy oils can be divided into two types on the basis of their origin that are primary heavy oils (immature heavy oils) and heavy oils formed due to water washing and biodegradation.[16] The role of biodegradation is supported by different GC−MS traces for oils from the E*j* and E*w* formations. The crude oils from the WZ57 oil field are considered to be immature heavy oils, which is suggested by lower C_{27} 18α(H)-22,29,30-trisnorneohopane/(C_{27} 18α(H)-22,29,30-trisnorneohopane + C_{27} 17α(H)-22,29,30-trisnorhopane) [Ts/(Ts + Tm)] ratios (<0.45) (Figure 3c). Although there is no obvious correlation between the density of oils and

https://doi.org/10.1021/acsomega.2c02826
ACS Omega 2022, 7, 24795−24811

Table 3. Summary of GC−MS Parameters of Saturated Fractions for Crude Oils in the Sub-Sag A, Weixinan Sag, BBW Basin[a]

no.	well	depth (m)	P1	P2	P3	P4	P5	P6	P7	P8	P9	P10	P11	P12
S01	WZ571	2820.9	0.62	0.33	2.96	1.56	1.75	1.44	0.62	2.42	0.11	0.25	1.45	3.50
S02	WZ571	2831.9	1.15	0.75	1.09	1.56	1.71	1.13	0.64	2.02	0.14	0.29	1.28	3.35
S03	WZ1113	995.5	n.d	n.d	n.d	n.d	n.d	7.50	6.68	1.10	0.21	0.34	0.80	2.01
S04	WZ111E1	986	n.d.	n.d.	n.d.	n.d.	n.d.	n.d.	n.d.	n.d.	0.18	0.34	0.78	1.89
S05	WZ111E1	991	n.d.	n.d.	n.d.	n.d.	n.d.	n.d.	n.d.	n.d.	0.21	0.35	0.79	2.01
S06	WZ111E1	995	n.d.	n.d.	n.d.	n.d.	n.d.	n.d.	n.d.	n.d.	0.20	0.36	0.76	1.92
S07	WZ111N3	2097.25	1.25	0.80	0.79	1.11	1.09	0.56	0.43	1.36	0.17	0.28	0.51	0.66
S08	WZ111N4	2088.25	1.56	0.98	0.59	1.11	1.08	0.41	0.30	1.40	0.22	0.27	0.55	0.72
S09	WZ111W2d	1582.04	0.95	0.73	0.90	1.07	1.08	0.46	0.30	1.73	0.22	0.24	0.73	2.20
S10	WZ111W2d	1551.01	0.96	0.78	0.82	1.09	1.05	0.48	0.31	1.74	0.20	0.29	0.71	2.21
S11	WZ61S1	1808	1.74	0.94	0.59	1.11	1.08	0.46	0.33	1.43	0.22	0.29	0.56	0.66
S12	WZ61S1	1812.1	1.35	0.91	0.72	1.11	1.09	0.46	0.34	1.44	0.22	0.29	0.62	0.78
S13	WZ61S1	1972.8	1.43	0.79	0.76	1.10	1.09	0.50	0.36	1.44	0.19	0.30	0.50	0.57
S14	WZ61S1	1991.3	1.55	0.81	0.71	1.11	1.09	0.48	0.34	1.45	0.19	0.30	0.48	0.55
S15	WZ1031	2033	1.31	0.81	0.76	1.08	1.05	0.45	0.28	1.65	0.26	0.41	0.38	0.59
S16	WZ103S1	2286.5	1.20	0.89	0.70	1.09	1.07	0.55	0.34	1.88	0.24	0.48	0.71	2.39
S17	WZ103W2	2104.5	1.03	0.67	0.93	1.07	1.09	0.44	0.23	2.09	0.22	0.45	0.37	0.56
S18	WZ1112	2856.1	1.05	0.71	0.94	1.08	1.05	0.41	0.25	1.68	0.32	0.34	0.42	0.59
S19	WZ611	1967	1.52	1.05	0.57	1.07	1.05	0.29	0.21	1.50	0.24	0.45	0.30	0.41

no.	well	P13	P14	P15	P16	P17	P18	P19	P20	P21	P22	P23	P24	P25
S01	WZ571	0.04	0.37	0.03	0.23	0.10	0.37	0.50	0.86	1.35	0.20	0.15	0.36	0.65
S02	WZ571	0.06	0.42	0.04	0.25	0.09	0.39	0.52	0.87	1.36	0.25	0.18	0.32	0.75
S03	WZ1113	0.06	0.56	0.07	0.26	0.05	0.44	0.55	0.89	1.00	0.38	0.37	0.08	2.15
S04	WZ111E1	0.05	0.57	0.06	0.27	0.05	0.44	0.55	0.88	1.02	0.34	0.32	0.08	2.11
S05	WZ111E1	0.06	0.57	0.07	0.26	0.06	0.44	0.55	0.89	1.00	0.37	0.37	0.08	2.22
S06	WZ111E1	0.05	0.56	0.07	0.27	0.04	0.45	0.56	0.87	1.01	0.35	0.31	0.08	2.06
S07	WZ111N3	0.05	0.52	0.05	0.26	0.03	0.40	0.59	0.89	0.98	0.36	0.33	0.09	2.21
S08	WZ111N4	0.06	0.55	0.07	0.28	0.04	0.41	0.57	0.89	1.03	0.36	0.28	0.10	1.88
S09	WZ111W2d	0.06	0.55	0.04	0.29	0.03	0.37	0.59	0.88	0.94	0.30	0.59	0.08	1.09
S10	WZ111W2d	0.07	0.53	0.04	0.28	0.04	0.39	0.58	0.89	0.80	0.32	0.59	0.09	1.01
S11	WZ61S1	0.07	0.57	0.05	0.27	0.06	0.44	0.58	0.88	1.10	0.38	0.35	0.10	1.29
S12	WZ61S1	0.07	0.57	0.05	0.27	0.05	0.45	0.59	0.88	1.06	0.36	0.35	0.10	1.27
S13	WZ61S1	0.06	0.59	0.06	0.28	0.05	0.43	0.58	0.89	1.00	0.39	0.39	0.09	1.61
S14	WZ61S1	0.06	0.57	0.05	0.26	0.05	0.40	0.58	0.89	1.01	0.37	0.37	0.10	1.66
S15	WZ1031	0.08	0.64	0.12	0.37	0.11	0.46	0.60	0.88	1.02	0.42	0.51	0.12	2.98
S16	WZ103S1	0.08	0.54	0.10	0.33	0.12	0.47	0.61	0.88	0.84	0.37	0.46	0.09	3.30
S17	WZ103W2	0.09	0.66	0.12	0.42	0.11	0.45	0.60	0.87	0.98	0.45	0.45	0.10	2.65
S18	WZ1112	0.13	0.85	0.31	0.61	0.27	0.51	0.59	0.86	0.41	0.49	0.51	0.19	2.51
S19	WZ611	0.08	0.67	0.13	0.40	0.10	0.49	0.62	0.89	0.66	0.42	0.49	0.11	2.57

[a](Parameters: P1 = $(nC_{21} + nC_{22})/(nC_{28} + nC_{29})$; P2 = nC_{21}^{-}/nC_{21}^{+}; P3 = TAR = $(nC_{27} + nC_{29} + nC_{31})/(nC_{15} + nC_{17} + nC_{19})$; P4 = $CPI_{22-32} = 2 \times (nC_{23} + nC_{25} + nC_{27} + nC_{29} + nC_{31})/(nC_{22} + 2 \times nC_{24} + 2 \times nC_{26} + 2 \times nC_{28} + 2 \times nC_{30} + nC_{32})$; P5 = OEP = $(nC_{25} + 6 \times nC_{27} + nC_{29})/(4 \times nC_{26} + 4 \times nC_{28})$; P6 = Pr/$nC_{17}$; P7 = Ph/$nC_{18}$; P8 = Pr/Ph; P9 = $C_{19}TT/(C_{19}TT + C_{23}TT) = C_{19}$ tricyclic terpane/(C_{19} tricyclic terpane + C_{23} tricyclic terpane); P10 = ETR = $(C_{28}TT + C_{29}TT)/(C_{28}TT + C_{29}TT + Ts)$; P11 = $C_{24}TeTT/C_{23}TT$; P12 = $C_{24}TeTT/C_{26}TT$; P13 = GA/$C_{30}H$ = gammacerane/C_{30} $\alpha\beta$ hopane; P14 = Ts/(Ts + Tm); P15 = C_{30} diahopane/(C_{30} diahopane + $C_{30}H$); P16 = $C_{29}Ts/(C_{29}Ts + C_{29}H)$; P17 = oleanane/$C_{30}H$; P18 = C_{31} homohopane/C_{30} $\alpha\beta$ hopane; P19 = C_{31} 22S/

https://doi.org/10.1021/acsomega.2c02826
ACS Omega 2022, 7, 24795−24811

Table 3. continued

(22S + 22R) homohopanes; P20 = C_{30} $\alpha\beta/(\alpha\beta + \beta\alpha)$ hopane; P21 = C_{27}/C_{29} = C_{27} ($\alpha\alpha\alpha$ 20S + $\alpha\beta\beta$ 20R + $\alpha\beta\beta$ 20S + $\alpha\alpha\alpha$ 20R) steranes/C_{29} ($\alpha\alpha\alpha$ 20S + $\alpha\beta\beta$ 20R + $\alpha\beta\beta$ 20S + $\alpha\alpha\alpha$ 20R) steranes; P22 = $\beta\beta$-C_{29}/$\sum C_{29}$(%) = C_{29} $\alpha\beta\beta$ sterane/(C_{29} $\alpha\alpha\alpha$ sterane + C_{29} $\alpha\beta\beta$ sterane); P23 = C_{29} $\alpha\alpha\alpha$ 20S/(20S + 20R) sterane; P24 = St/H = steranes/hopanes = C_{27}−C_{29} regular steranes/C_{29}−C_{35} $\alpha\beta$ hopanes; P25 = 4-MSI = C_{30} 4-methylsteranes/C_{29} regular steranes; and n.d. = not applicable).

burial depth (Figure 3b), the negative relationship between density and Ts/(Ts + Tm) indicates that the density of crude oils decreases with increasing thermal maturity (Figure 3c). As shown in Figure 3d, the density has a negative correlation with the stable carbon isotope ratios of oils, suggesting the differences in density are related to the source material of OM, and the oils are derived from different source rocks.

Collectively, the variation of physical properties implies that thermal maturity decreases from group A3 to group A1, except the biodegraded oils in the A2 oil family. Besides that, it suggests that they are probably derived from different source rocks.

4.1.2. Stable Carbon Isotopic Composition of Oils. The stable isotopic composition of crude oil has been used for many decades to provide information on relationships between oil families. The stable carbon isotope ratios ($\delta^{13}C$) of the whole oils, saturated and aromatic hydrocarbon, nitrogen-, sulfur- and oxygen-bearing compounds (NSO), and the asphaltene fraction from the three oil families are presented in Table 2. The $\delta^{13}C$ values of the whole oils in different oil families have obvious differences. Group A1 has much more negative $\delta^{13}C_{oil}$ (whole oil) values (average = −29.55‰), $\delta^{13}C_{sat}$ (saturated hydrocarbon) values (average = −31.13‰), and $\delta^{13}C_{aro}$ (aromatic hydrocarbon) values (average = −28.7‰) than groups A2 ($\delta^{13}C_{oil}$ average of −26.98‰; $\delta^{13}C_{sat}$ average of −27.59‰; $\delta^{13}C_{aro}$ average of −25.95‰) and A3 ($\delta^{13}C_{oil}$ average of −25.33‰; $\delta^{13}C_{sat}$ average of −25.55‰; $\delta^{13}C_{aro}$ average of −23.89‰). A plot of the $\delta^{13}C_{sat}$ versus $\delta^{13}C_{aro}$ shows that groups A1, A2, and A3 fall into three clusters (Figure 4a). These values indicate that studied oil families are originated from multiple source rocks.

To our knowledge, the $\delta^{13}C$ variation is dependent on some factors, such as biological OM, the depositional condition,[17,18] thermal maturity, and biodegradation.[19,20] Just to get a better understanding of its effectiveness for oil family classification, these controlling factors are discussed below.

Biodegradation does have a minor influence on $\delta^{13}C_{sat}$ and a small effect on the $\delta^{13}C_{whole}$.[21] Marcano et al.[22] also suggested biodegradation on crude oil does not lead to significant carbon variations. The biodegraded oil samples are mainly from group A2, and their $\delta^{13}C$ of the whole oil, saturate, and aromatic fractions ranges from −26.79 to −26.50‰ (average −26.62‰), −27.40 to −27.10‰ (average −27.19‰), and −26.10 to −24.74‰ (average −25.41‰), respectively. The difference between the biodegraded oils and other oils in the A2 group is less than 1‰ (Table 2), suggesting biodegradation has no significant effect on stable carbon isotope in this study area.

The influence of thermal maturity on the stable carbon isotope will make it much heavier (less negative) due to the preferential cleavage of ^{12}C−^{12}C bonds.[19] As shown in Figure 4b, the inconspicuous positive relationship (R^2 = 0.42) between the stable carbon isotopic composition of the whole oil and Ts/(Ts + Tm) suggested that it is likely less affected by thermal maturity. It seems to mean that the thermal maturity of the A1 oil family is lower than those of A2 and A3 families. However, because thermal maturity can only account for minor $\delta^{13}C$ variations (usually <1‰), the huge difference (the deviation exceeds 3‰) between A1 and A3 is not entirely the result of thermal maturity in this study area.

Although numerous studies on the carbon isotope analysis have been done to identify the lacustrine and marine OM, the isotopic variations of the OM are still unclear. In general, oils

https://doi.org/10.1021/acsomega.2c02826
ACS Omega 2022, 7, 24795−24811

Table 4. Rock-Eval Parameters and Carbon Isotopes of Kerogen of the Shale Samples from the Weixinan Sag[a]

hydrocarbon supply combination	TOC (%)	PG (mg/g)	T_{max} (°C)	HI (mg/g)	$\delta^{13}C_{PDB}$ (‰)
SR1	0.84−9.03/2.92	2.43−44.11/13.9	381−446/430	147−823/394	−29.13−26.10/−27.83
SR2	0.33−2.74/1.92	0.55−12.23/6.96	379−448/435	115−464/307	−30.14−26.10/−28.14
SR3	0.58−10.03/3.77	1.24−89.68/15.54	372−446/437	91−862/333	−27.52−21.22/−25.93

[a](Note: TOC = total organic carbon; PG = S_1 +S_2 (mg/g); HI = S_2/TOC (mg/g); T_{max} = temperature of maximum hydrocarbon generation rate; and HI = S_2/total organic carbon. Each cell consists of two parts: above the horizontal line is the range (minimum to maximum) and below is the average).

generated from terrigenous OM are isotopically less negative than marine oils with $\delta^{13}C_{oil}$ > −26‰. On the contrary, a study reported by Sun et al.[23] has concluded that marine oils are isotopically more negative than nonmarine oils, and the heavy carbon isotope composition is related to the development of specific algae. As shown in Figure 4c, the positive relationship (R^2 = 0.74) between $\delta^{13}C_{whole}$ and the ratio of C_{30} 4-methylsterane to C_{29} regular steranes (4-MSI) implies that the less-negative $\delta^{13}C_{whole}$ is closely related to algal bloom even though the samples are in various maturity stages. It is coincident with the results reported for the Pearl River Mouth, Bohaiwan, Sunda basins.[23−26] The deposits in these basins are formed in a freshwater environment with abundant C_{30} 4-methylsterane. Thus, in these studied oils, the $\delta^{13}C_{whole}$ values of the A1 and A2 oils are mostly less than −26‰, suggesting that algae have a contribution on the biological sources of their source rocks. However, the relatively heavy $\delta^{13}C_{whole}$ values (>−26‰) in the A3 oils may reveals the algal bloom, especially the dinoflagellate.

In summary, the differences in stable carbon isotopic compositions among the groups of oil are consistent with biological source and thermal maturity variations (Figure 4b,c). There is a clear trend in the bulk carbon isotope values, suggesting thermal maturity decreasing from group A3 to group A1 and the algal bloom increasing from group A3 to group A1 as well.

4.1.3. Aliphatic Hydrocarbon. 4.1.3.1. n-Alkanes and Isoprenoids. The *n*-alkane distributions are widely used to distinguish sources of OM and evaluate the thermal maturity of crude oils and source rocks.[27,28] GC−MS analyses performed on saturated hydrocarbons of the sub-sag A oils show that the carbon number of the *n*-alkanes ranges from C_{10} to C_{40} (Figure 5). Histograms representing the distributions are shown in Figure 5, but four samples (S03, S04, S05, and S06) from the A2 oil family showed slight biodegradation and has been excluded from Figure 5. *n*-alkanes in the crude oils fall into two patterns (Figure 5). Pattern 1 is a strong odd-over-even predominance, with maxima at nC_{27} (Figure 5a), for the A1 oil family. Pattern 2 is characterized by a slight odd-over-even predominance, with a maximum at nC_{17}, nC_{23}, or nC_{25}, for the oils from the groups A2 and A3 (Figure 5b,c). The OEP $[(nC_{25} + 6 \times nC_{27} + nC_{29})/(4 \times nC_{26} + 4 \times nC_{28})]$ values (average 1.56; Table 3) and CPI $[2 \times (nC_{23} + nC_{25} + nC_{27} + nC_{29} + nC_{31})/(nC_{22} + 2 \times nC_{24} + 2 \times nC_{26} + 2 \times nC_{28} + 2 \times nC_{30} + nC_{32})]$ values (average = 1.73; Table 3) suggest a low thermal maturity of A1 oils. The OEP and CPI values of the oils from the A2 and A3 groups are around 1.0 (Table 3), indicating that they are in the mature−high mature stage. However, closer observation of the data suggests that the oils from the A3 group are slightly more mature than the oils from the A2 group.

The terrestrial/aquatic ratio (TAR), which is defined as $(nC_{27} + nC_{29} + nC_{31})/(nC_{15} + nC_{17} + nC_{19})$,[27] is in the range of 1.09−2.96 (average = 2.03) in the A1 oil family compared to the A2 oil family (0.59−0.90; average 0.73) and the A3 oil family (0.57−0.94; average 0.78). Excluding the influence of thermal maturity on the TAR ratios (Figure 6a), it possibly indicates that the A1 was derived from a source rock with a larger input of terrigenous OM (e.g., higher plants) compared to the A2 and A3 oils. In comparison, the source rock of A2 and A3 oil groups was deposited with algal OM. The (n-C_{21}^-/n-C_{22}^+) ratios lie in the range of 0.33−0.75 (average = 0.54) in the oils from the A1 group, which are lower than those in the A2 oil family (0.73−0.98; average 0.84) and the A3 oil family (0.67−1.05; average 0.83).

Pristane/phytane (Pr/Ph) is commonly used to evaluate redox conditions during deposition, although it is also affected by thermal maturation.[29−31] As shown in Figure 6b, there is no positive and/or negative relationship between Pr/Ph and Ts/(Ts + Tm), suggesting the thermal maturity has no obvious influence on the Pr/Ph ratios. Generally, the low Pr/Ph (<0.6) indicates the hypersaline environment of the source rock, Pr/Ph < 0.8 represents anoxic conditions, and Pr/Ph > 3.0 is interpreted to be an indicator for an oxic environment with the input of terrestrial OM.[32,33] The Pr/Ph ratios of most of the analyzed oils are >1 (1.10−2.42; average = 1.64; Table 3), suggesting these oils were derived from a source rock deposited in an oxidizing environment. Comparatively speaking, the sedimentary environment of the A3 and A2 oils is more reductive than that of the A1 oils (Figure 7b,c). The Pr/nC_{17} and Ph/nC_{18} ratios of the A1 oils are higher than those of the A2 and A3 oils, except for samples S03 in which Pr/nC_{17} and Pr/nC_{18} are highest due to biodegradation. The cross plot of Pr/nC_{17} and Pr/nC_{18} (Figure 7a) indicates that most of oils from these three families originated mixed OM, except for the A1 oils with a certain terrestrial OM. Besides that, the Pr/nC_{17} and Ph/nC_{18} ratios decrease with increasing thermal maturity, suggesting the A3 oils are more mature than A2 and A1(Figure 7a).

4.1.3.2. Terpanes. In compared to the hopanes, tricyclic terpanes have a relatively low abundance (Figure 8). However, a relatively high abundance of tricyclic terpanes was detected in the A3 oil group compared to a moderate abundance in the A2 oils and a low concentration in the A1 oils. Tricyclic terpanes have a variety of origins, such as Tasmanites,[34] bacteria,[35,36] and higher plants.[37] Generally, the $C_{19}TT/(C_{19}TT + C_{23}TT)$ was widely used as an effective indicator for the terrigenous OM input in low-mature sediments.[38,39] However, as shown in Figure 6c, a strong positive relationship between $C_{19}TT/(C_{19}TT + C_{23}TT)$ and Ts/(Ts + Tm) (R^2 = 0.80) suggests that it is strongly affected by thermal maturity. The $C_{19}TT/(C_{19}TT + C_{23}TT)$ ratios are in the range of 0.11−0.14 (average = 0.13), 0.17−0.22 (average = 0.20), and 0.22−0.32 (average = 0.26) in the A1, A2, and A3 oil families, respectively. It suggests that A3 oils have higher thermal maturity than A2 and A1 oils. The extended tricyclic ratio

https://doi.org/10.1021/acsomega.2c02826
ACS Omega 2022, 7, 24795−24811

Table 5. Summary of GC−MS Parameters of Saturated Fractions for Source Rocks from the SR1 and SR3 in the Sub-Sag A, Weixinan Sag, BBW Basin[a]

well	depth (m)	combination	PP1	PP2	PP3	PP4	PP5	PP6	PP7	PP8	PP9	PP10	PP11	PP12	PP13	PP14	PP15	PP16	PP17	PP18	PP19	PP20	PP21	PP22
WZ592	3127	SR1	1.42	0.52	1.44	1.56	1.51	0.58	0.38	1.32	n.d.	n.d	n.d	0.01	0.35	0.27	0.04	0.05	1.50	0.87	0.13	0.67	0.04	n.d.
WZ592	3145	SR1	0.67	0.57	1.44	1.64	1.88	0.82	0.76	1.44	0.20	n.d	n.d	0.01	0.54	0.31	0.02	0.05	1.43	0.91	0.11	0.68	0.06	n.d.
WZ592	3158	SR1	0.92	0.38	2.20	1.42	1.45	1.74	0.83	1.95	n.d.	n.d	n.d	n.d.	0.36	0.25	0.03	0.05	1.57	0.79	0.16	0.64	0.03	n.d.
WZ592	3270	SR1	0.57	0.37	2.31	1.32	1.28	1.43	0.79	2.02	0.53	n.d	n.d	0.01	0.46	0.30	0.04	0.07	1.70	0.82	0.12	0.76	0.05	n.d.
WZ592	3272	SR1	0.73	0.39	2.06	1.29	1.28	1.37	0.72	1.98	n.d	0.54	0.14	0.01	0.41	0.27	0.04	0.08	1.78	0.79	0.10	0.77	0.05	n.d.
WZ592	3310	SR1	0.74	0.55	1.30	1.33	1.34	1.81	0.85	2.47	n.d	0.00	0.14	0.00	0.34	0.16	0.61	0.08	1.60	0.74	0.12	0.70	0.08	n.d.
WZ592	3312.6	SR1	1.04	0.53	1.01	0.78	0.71	1.00	0.31	3.59	0.63	0.00	0.18	0.01	0.40	0.13	2.35	0.10	1.35	0.67	0.13	0.73	0.11	n.d.
WZ592	3320	SR1	0.86	0.54	1.36	1.49	1.46	2.48	0.82	3.37	n.d	0.00	n.d	0.01	0.40	0.25	0.28	0.05	1.38	0.94	0.14	0.66	0.06	n.d.
WZ592	3332	SR1	0.96	0.55	1.35	1.28	1.35	0.94	0.35	2.85	n.d	0.00	0.08	0.01	0.60	0.23	0.02	0.10	1.76	0.93	0.11	0.79	0.05	n.d.
WZ592	3394	SR1	1.24	0.57	1.18	1.31	1.18	1.07	0.54	1.97	n.d	0.00	0.10	0.01	0.47	0.14	0.01	0.07	1.64	0.74	0.22	0.65	0.04	n.d.
WZ112N1D	2828	SR1	0.91	1.34	0.56	1.35	1.39	2.41	1.43	1.19	n.d.	n.d.	n.d.	0.10	0.31	0.16	0.13	0.43	1.11	1.44	0.24	0.04	n.d.	n.d.
WZ592	3460	SR1	1.24	0.63	1.04	1.32	1.22	0.82	0.40	2.01	n.d.	0.00	0.06	0.01	0.69	0.29	0.02	0.07	1.59	0.87	0.26	0.72	0.03	n.d.
WZ571	2884	SR1	1.25	0.66	1.15	1.65	1.81	1.30	0.83	1.64	0.39	0.00	0.00	n.d.	0.39	0.33	0.08	0.14	0.89	1.04	0.37	n.d.	0.11	0.36
WZ571	2964	SR1	1.47	0.77	0.92	1.62	1.66	1.12	0.53	2.44	0.44	0.00	0.00	n.d.	0.44	0.40	0.12	0.16	1.02	1.64	0.37	n.d.	0.10	0.48
WZ571	3210	SR1	1.70	0.83	0.79	1.50	1.50	1.69	0.62	3.08	0.44	0.00	0.00	n.d.	0.44	0.31	0.08	0.21	1.24	1.19	0.32	0.43	0.06	0.69
WZ1121	2984	SR1	1.98	0.92	0.62	1.26	1.16	1.51	0.53	3.14	0.16	0.06	0.06	n.d.	0.16	0.09	0.07	0.25	1.34	0.65	0.45	0.48	0.08	0.37
WZ1121	3242	SR3	1.65	0.81	0.71	1.15	1.12	0.71	0.42	1.72	0.87	0.08	0.08	n.d.	0.87	0.48	0.18	0.22	1.10	0.83	0.45	0.63	0.11	1.46
WZ1121	3326	SR3	1.87	1.21	0.42	1.08	1.05	0.36	0.26	1.56	0.93	0.18	0.18	n.d.	0.93	n.d	n.d.	0.26	1.18	1.19	0.44	0.34	0.25	1.07
WZ1121	3344	SR3	1.23	0.53	1.20	1.09	1.07	0.62	0.48	1.23	0.90	0.27	0.27	n.d.	0.90	0.71	0.21	0.27	0.96	0.95	0.42	0.66	0.22	1.56
WZ1121	3402	SR3	0.94	0.36	2.10	1.07	1.05	1.12	0.79	1.21	0.96	1.14	1.14	n.d.	0.96	0.88	n.d.	0.15	0.79	0.57	0.50	0.54	0.73	2.52

[a](Note: PP1 = $(nC_{21} + nC_{22})/(nC_{28} + nC_{29})$; PP2 = nC_{21}^{-}/nC_{21}^{+}; PP3 = TAR = $(nC_{27} + nC_{29} + nC_{31})/(nC_{15} + nC_{17} + nC_{19})$; PP4 = $CPI_{22-32} = 2 \times (nC_{23} + nC_{25} + nC_{27} + nC_{29} + nC_{31})/(nC_{22} + 2 \times nC_{24} + 2 \times nC_{26} + 2 \times nC_{28} + 2 \times nC_{30} + nC_{32})$; PP5 = OEP = $[(nC_{25} + 6 \times nC_{27} + nC_{29})/(4 \times nC_{26} + 4 \times nC_{28})]$; PP6 = Pr/$nC_{17}$; PP7 = Ph/$nC_{18}$; PP8 = Pr/Ph; PP9 = C_{19}TT/(C_{19}TT + C_{23}TT) = C_{19} tricyclic terpane/(C_{19} tricyclic terpane + C_{23} tricyclic terpane); PP10 = ETR = (C_{28}TT + C_{29}TT)/(C_{28}TT + C_{29}TT + Ts); PP11 = C_{24}TeTT/C_{23}TT; PP12 = GA/C_{30}H = gammacerane/C_{30} $\alpha\beta$ hopane; PP13 = Ts/(Ts + Tm); PP14 = C_{29}Ts/(C_{29}Ts + C_{29}H); PP15 = oleanane/C_{30}H; PP16 = C_{31} 22R homohopane/C_{30} $\alpha\beta$ hopane; PP17 = C_{31} 22S/22R homohopanes; PP18 = C_{27}/C_{29} = C_{27} ($\alpha\alpha\alpha$ 20S + $\alpha\beta\beta$ 20R + $\alpha\beta\beta$ 20S + $\alpha\alpha\alpha$ 20R) steranes/C_{29} ($\alpha\alpha\alpha$ 20S + $\alpha\beta\beta$ 20R + $\alpha\beta\beta$ 20S + $\alpha\alpha\alpha$ 20R) steranes; PP19 = $\beta\beta$-$C_{29}/\sum C_{29}$(%) = C_{29} $\alpha\beta\beta$ sterane/(C_{29} $\alpha\alpha\alpha$ sterane + C_{29} $\alpha\beta\beta$ sterane); PP20 = C_{29} $\alpha\alpha\alpha$ 20S/(20S + 20R) sterane; PP21 = St/H = steranes/hopanes = C_{27}−C_{29} regular steranes/C_{29}−C_{35} $\alpha\beta$ hopanes; PP22 = 4-MSI = C_{30} 4-methylsteranes/C_{29} regular steranes; and n.d. = not applicable.

https://doi.org/10.1021/acsomega.2c02826
ACS Omega 2022, 7, 24795−24811

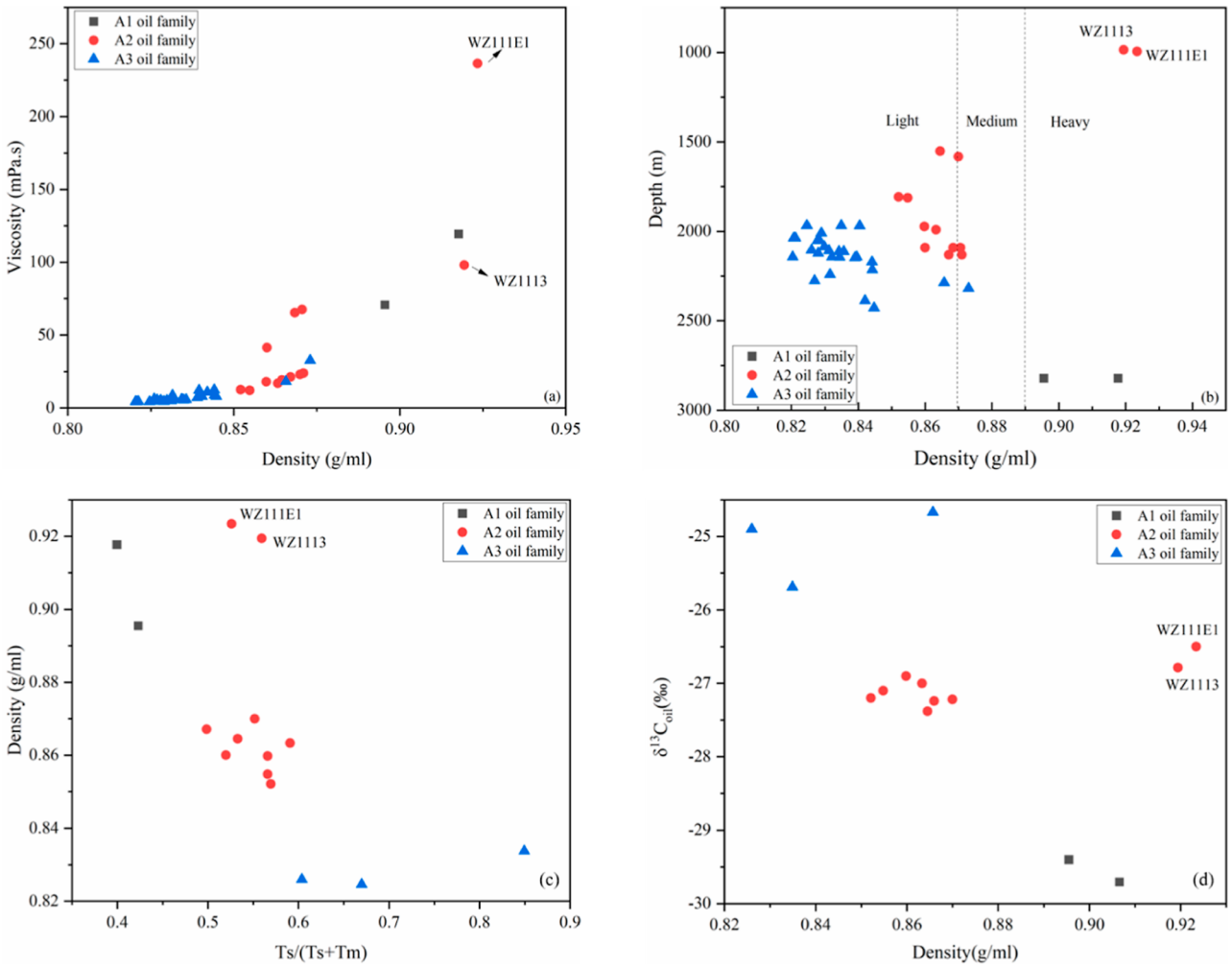

Figure 3. Scatter plots of (a) density vs viscosity, (b) density vs depth, (c) density vs Ts/(Ts + Tm), and (d) density vs stable carbon isotope values ($\delta^{13}C_{oil}$) of crude oils in the sub-sag A of the Weixinan sag.

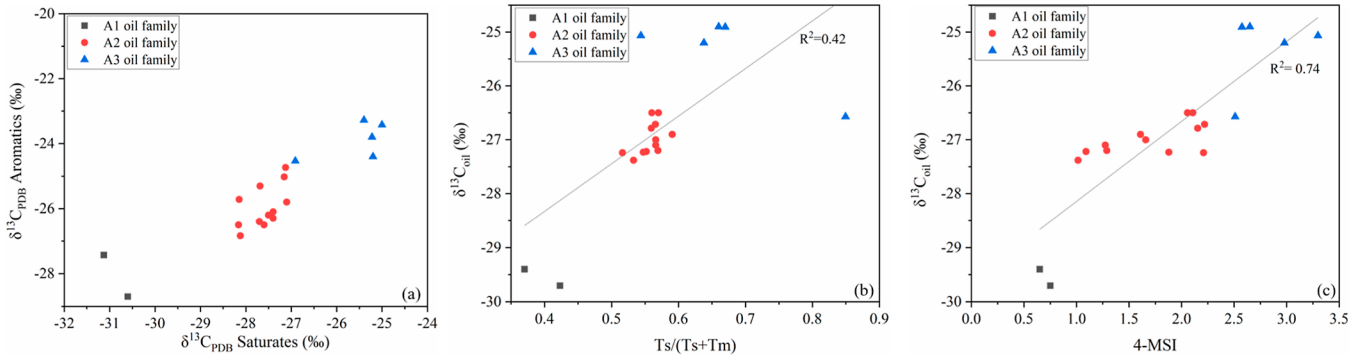

Figure 4. Cross plots of (a) $\delta^{13}C_{PDB}$ saturates vs $\delta^{13}C_{PDB}$ aromatics, (b) $\delta^{13}C_{oil}$ vs Ts/(Ts + Tm), and (c) 4-MSI vs $\delta^{13}C_{oil}$ of three oil families in the sub-sag A, Weixinan Depression.

(ETR) has the ratio of 0.25−0.29 (average = 0.27), 0.26−0.34 (average = 0.31), and 0.34−0.48 (average = 0.43) in the A1, A2, and A3 oil families, respectively. It implies that their source rocks are derived from the freshwater environment because the ETR is widely used for an effective indicator of salinity.[40,41] C_{24} tetracyclic terpane/C_{23} tricyclic ($C_{24}Te/C_{23}TT$) is also an index for terrestrial OM.[42,43] The amount of $C_{24}Te$ is slightly higher with $C_{24}Te/C_{23}TT$ varying in a range of 1.25−1.42 (average 1.36) in the A1 oil family compared to that in the A2 oil family (0.48−0.8; average = 0.65; Table 3) and A3 oil family (0.30−0.71; average = 0.44; Table 3). It is consistent with the results from the TAR, suggesting a larger input of terrigenous OM to the source rocks of the A1 oil family than those of A2 and A3 oil families.

A series of C_{27}−C_{35} hopanes, except for C_{28} homologue, are present in the crude oils. The oils from the A1 and A2 oil families have a relatively low oleanane/C_{30} $\alpha\beta$ hopane ratio (0.03−0.1; average = 0.05), while the oleanane/C_{30} $\alpha\beta$ hopane

https://doi.org/10.1021/acsomega.2c02826
ACS Omega 2022, 7, 24795−24811

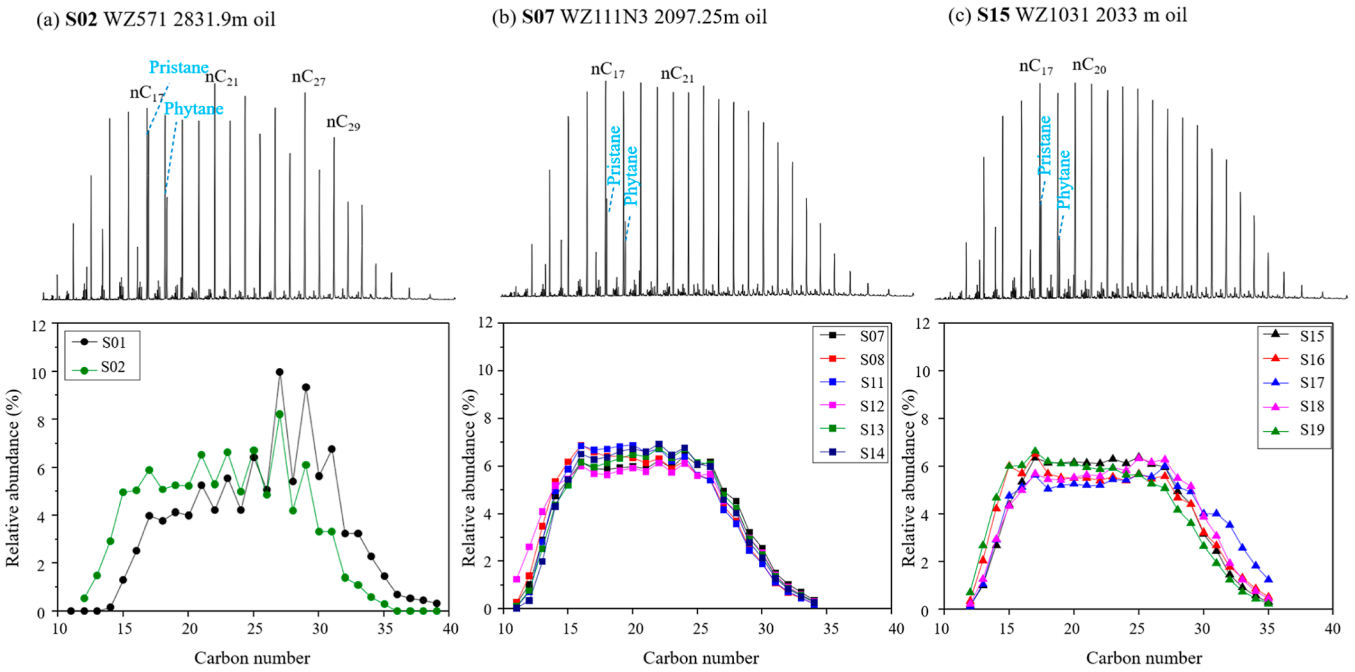

Figure 5. Mass chromatograms (m/z 85) of saturated hydrocarbon fractions of representative crude oils and normalized n-alkane profiles from (a) A1 oil family, (b) A2 oil family, and (c) A3 oil family in the sub-sag A of the Weixinan sag. Relative abundance = $C_i/\sum C_i \times 100\%$ (i = 10−40).

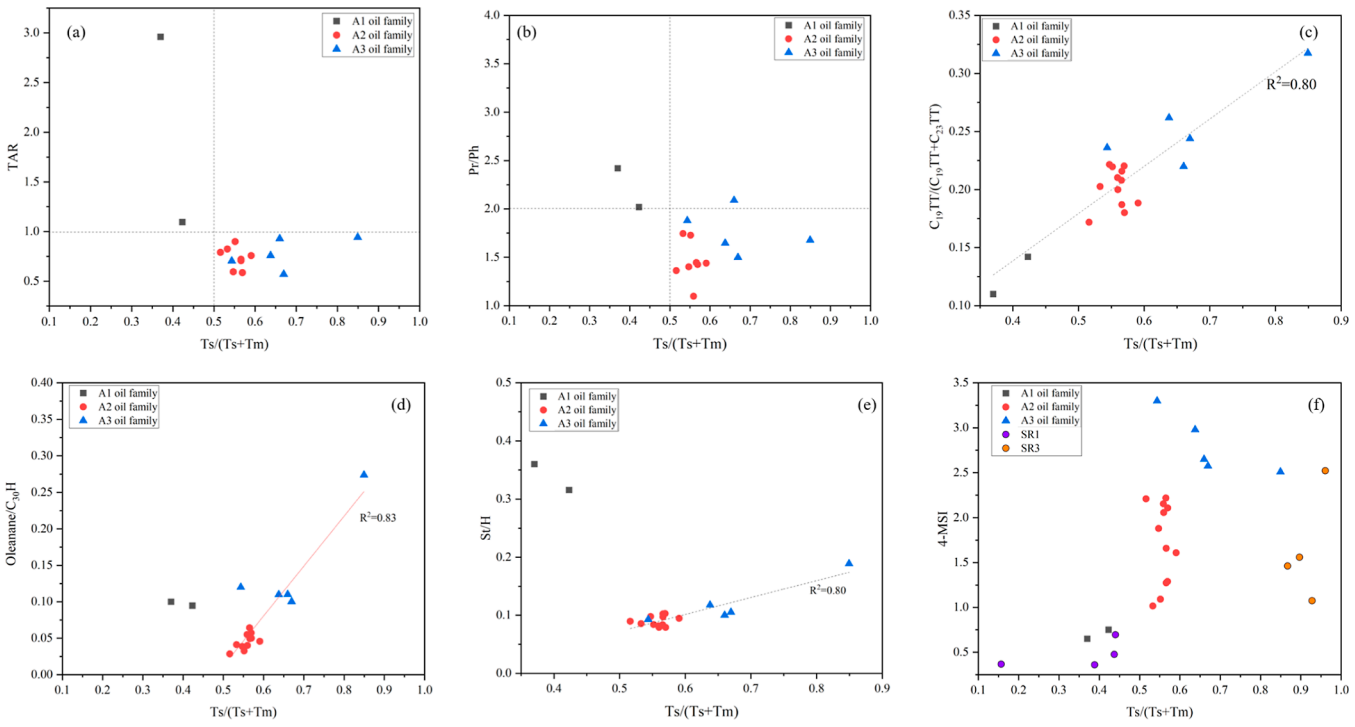

Figure 6. Scatter plots of (a) TAR vs Ts/(Ts + Tm), (b) Pr/Ph vs Ts/(Ts + Tm), (c) $C_{19}TT/(C_{19}TT + C_{23}TT)$ vs Ts/(Ts + Tm), (d) oleanane/$C_{30}H$ vs Ts/(Ts + Tm), (e) St/H vs Ts/(Ts + Tm), and (f) 4-MSI vs Ts/(Ts + Tm), showing the influence of thermal maturity on the geochemical parameters. (Note: St/H represents steranes/hopanes = C_{27}−C_{29} regular steranes/C_{29}−C_{35} $\alpha\beta$ hopanes; 4-MSI = the ratio of C_{30} 4-methylsterane to C_{29} regular steranes.)

ratio of the A3 oil group is >0.1 (0.10−0.27, average = 0.14). A high oleanane/C_{30} $\alpha\beta$ hopane ratio may imply the contribution of gymnosperms to the OM. Nevertheless, good exponential correlation between oleanane/C_{30} $\alpha\beta$ hopane and Ts/(Ts + Tm) (R^2 = 0.83), except for the A1 oil family, shows that the oleanane/C_{30} $\alpha\beta$ hopane ratio increases with increasing thermal maturity (Figure 6d). This is consistent with the studies of Ekweozor and Telnaes[44] and Tyson[45] who suggested the oleanane/C_{30} $\alpha\beta$ hopane ratio increases from the low value in the immature sample to the maximum value at the top of the oil window and then remains relatively stable. The maturity-related parameters, including Ts/(Ts + Tm), C_{30} diahopane/(C_{30} diahopane + C_{30} $\alpha\beta$ hopane), $C_{29}Ts/(C_{29}Ts + C_{29}H)$, C_{31} homohopane/$C_{30}H$, and C_{30} $\alpha\beta/(\alpha\beta + \beta\alpha)$, indicate a

https://doi.org/10.1021/acsomega.2c02826
ACS Omega 2022, 7, 24795−24811

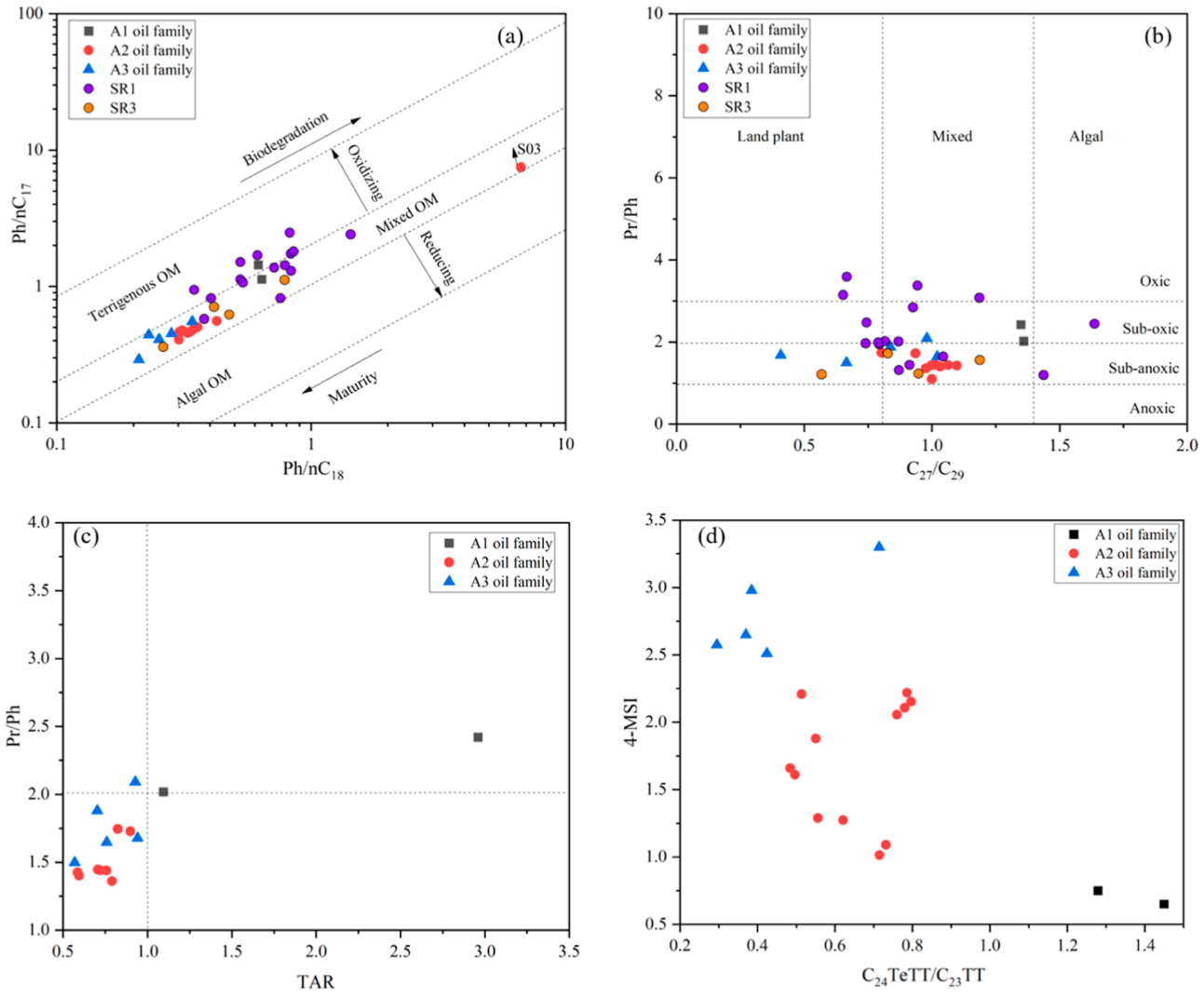

Figure 7. Cross plots of (a) Ph/nC_{18} vs Pr/nC_{17}, (b) C_{27}/C_{29} vs Pr/Ph, (c) TAR vs Pr/Ph, and (d) 4-MSI vs $C_{24}Te/C_{23}TT$. (Note: C_{27}/C_{29} = (5α(H),14α(H),17β(H) C_{27} sterane 20S + 5α(H),14β(H),17β(H) C_{27} sterane 20S + 5α(H),14β(H),17β(H) C_{27} sterane 20R + 5α(H),14α(H),17α(H) C_{27} sterane 20R)/(24-ethyl-5α(H), 14α(H), 17α(H)−C_{29} sterane 20S + 24-ethyl-5α(H), 14β(H), 17β(H)−C_{29} sterane 20R + 24-ethyl-5α(H), 14β(H), 17β(H)−C_{29} sterane 20S + 24-ethyl-5α(H), 14α(H), 17α(H)−C_{29} sterane20R); TAR = (nC_{27} + nC_{29} + nC_{31})/(nC_{15} + nC_{17} + nC_{19}); 4-MSI = the ratio of C_{30} 4-methylsterane to C_{29} regular steranes; and $C_{24}Te/C_{23}TT$ = C_{24} tetracyclic terpane/C_{23} tricyclic.)

trend in maturity from low to high variability in the A1, A2, and A3 oil families (Figure 9 and Table 3). Gammacerane is thought to be a good indicator of water column stratification and perhaps the salinity.[46] The gammacerane/C_{30} $\alpha\beta$ hopane ratio (Gam/C_{30}H) of the three oil families is <0.15 (0.04−0.0.13; average 0.07; Table 3), suggesting that they were originated in a freshwater environment with unstable water column stratification.

Overall, some source-indicative parameters about terpanes, such as $C_{19}/(C_{19}TT + C_{23}TT)$ and oleanane/C_{30} $\alpha\beta$ hopane, are apparently influenced by thermal maturity in the high-mature stage (Figure 6). Thus, they cannot be used for the assessment of OM sources for the A2 and A3 oil families in the study area, but they could reflect the increased thermal maturity from the A1 oils to A3 oils. However, the algal OM contributes more to the A3 oils than the A2 and A1 oils, which is supported by $C_{24}Te/C_{23}TT$ ratios.

4.1.3.3. Steranes. Regular steranes are commonly used for delineating the biological sources and thermal maturity of OM. The ratio of C_{27} steranes/C_{29} steranes in the A1 and A2 oils is mostly >1 (0.8−1.36, average = 1.05), which is higher than that in the A3 oil family (0.41−1.02, average = 0.78). The cross plot of Pr/Ph and C_{27}/C_{29} $\alpha\alpha\alpha$ 20R steranes, in which most of the oils are indicated to be sourced from mixed OM in a subanoxic environment, expect for the A1 oils is shown in Figure 7b. The C_{29} $\alpha\alpha\alpha$ 20S/(20S + 20R) sterane ratio ranges from 0.12 to 0.56, and the C_{29} $\alpha\beta\beta/(\alpha\beta\beta + \alpha\alpha\alpha)$ sterane ratio ranges from 0.40 to 0.54 (Table3). The C_{30} 4-methylsteranes are widely detected in the lacustrine deposits in eastern China.[47] Its biological precursors are related to certain algae, especially dinoflagellates.[48−50] Abundance C_{30} 4-methylstrane was detected in the A1, A2, and A3 oil families. The ratio of C_{30} 4-methylsteranes to C_{29} steranes (4-MSI) is in the range of 0.65−0.75 (average = 0.70), 1.01−2.22 (average = 1.71), and 2.51−3.30 (average = 2.80) in the A1, A2, and A3 oil families, respectively. It reveals a flourish of dinoflagellates in the lake during the deposition period of source rocks. Fu[11] proposed that the 4-MSI could be used for evaluation of OM, that is, high-quality shales (4-MSI > 1.5), good source rocks (4-MSI > 0.5), and fair source rocks (4-MSI < 0.5). Thus, it is concluded

https://doi.org/10.1021/acsomega.2c02826
ACS Omega 2022, 7, 24795−24811

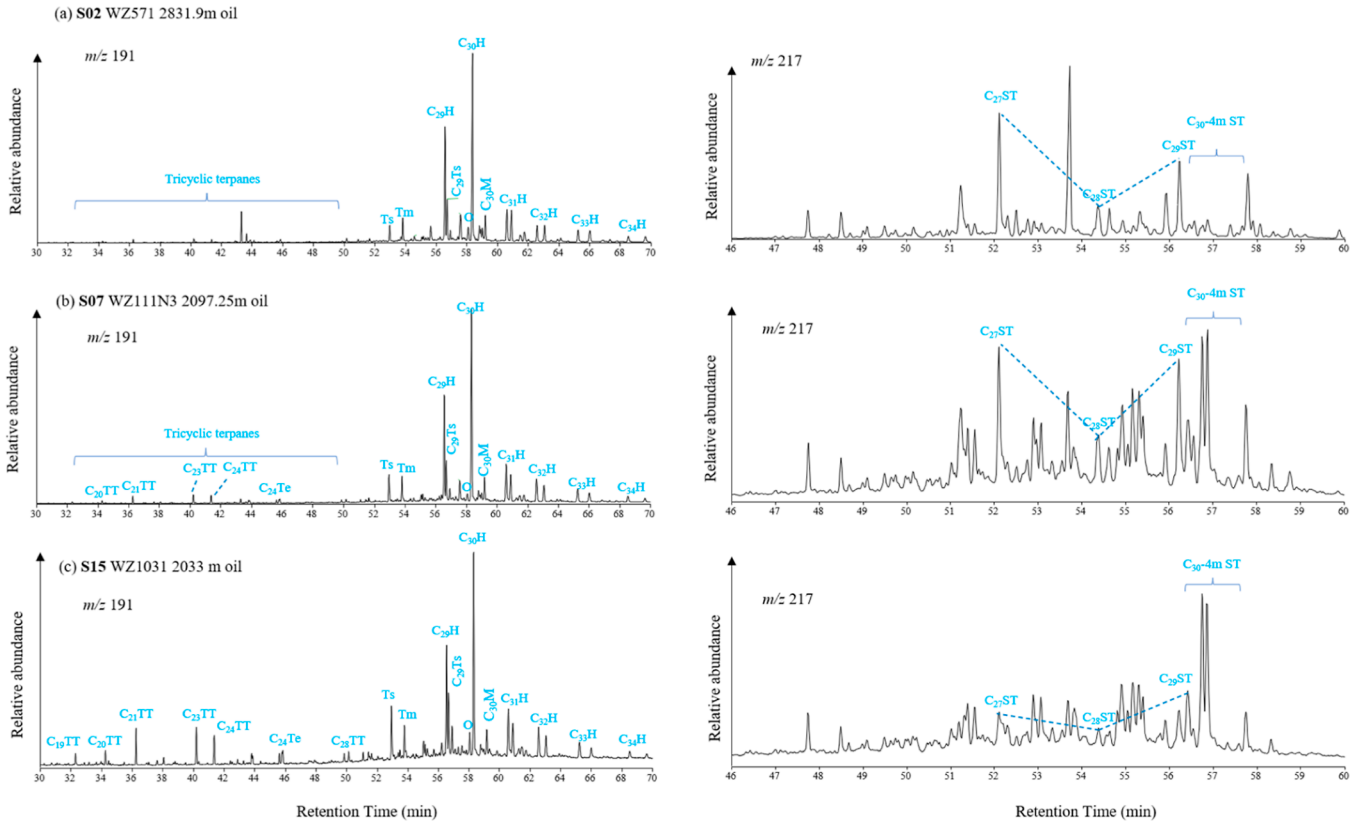

Figure 8. Representative m/z 191 and 217 mass chromatograms of the aliphatic hydrocarbon fraction showing the distribution of terpanes and steranes in the A1 (a), A2 (b), and A3 (c) oil families.

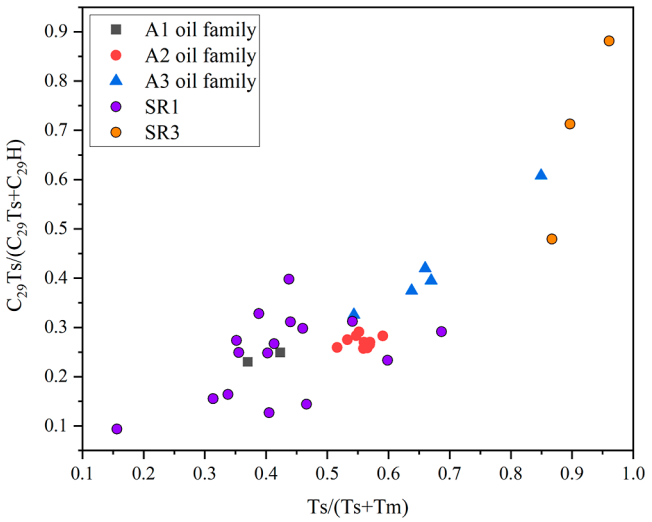

Figure 9. Cross plot of $C_{29}Ts/(C_{29}Ts + C_{29}H)$ vs $Ts/(Ts + Tm)$ for the oil families and source rocks in the sub-sag A of the Weixinan sag. SR1 = the upper hydrocarbon supply combination; SR3 = the lower hydrocarbon supply combination.

that the A1 oils were generated from the good source rocks, and A2 and A3 oils were derived from the excellent shales.

4.2. Geochemical Characteristics of Source Rocks. According to previous studies, the shales from the Liushagang Formation are the main source rock in the Weixinan sag, especially the second member of Liushagang Formation (El^2).[51−55] However, according to the results of Fu et al.[56] and Fu and Liu,[10] the quality of El^2 source rocks is quite different. Thus, there is a new definition, which is given for the division of source rocks from the Weixinan sag, based on the comprehensive investigation on geochemical analysis and regional sedimentary facies of source rocks. It is suggested that there were three sets of hydrocarbon supply assemblages of source rocks in the Weixinan sag: the first hydrocarbon supply assemblage includes the lower part of the El^1 and the upper part of the El^2 (the upper hydrocarbon supply assemblage; SR1); the second one, so-called the middle hydrocarbon supply assemblage (SR2), contains the middle part of the El^2 formation, and the last one consists of the lower part of the El^2 and the upper part of the El^3 (the lower hydrocarbon supply assemblage; SR3).[5,57] In our work, the discussion about the geochemical characteristics of source rocks is being carried out based on this new classification. After our preliminary analysis of the source rocks in the Weixinan sag, it is concluded that crude oils were generated from the source rocks located in the center of subsag and migrated into the reservoir for accumulation. Although the lack of drilling in the center of sub-sag A makes it an obstacle, it adjoins the sub-sag B which contains significant source rocks and they have similar sedimentary facies and history. Oil−source rock correlation was measured by studying the wells drilling the source strata in the edge of sub-sag A and sub-sag B.

4.2.1. Bulk Organic Geochemical Characteristics. The results of TOC and Rock-Eval pyrolysis of shales from the upper, middle, and lower hydrocarbon combinations are tabulated in Table 4 and plotted in Figure 10. It shows that the shales from the upper hydrocarbon combination (SR1) are fairly excellent source rocks, suggested by medium TOC values (0.84−9.03%; average = 2.92%) and medium PG (S_1 + S_2)

https://doi.org/10.1021/acsomega.2c02826
ACS Omega 2022, 7, 24795−24811

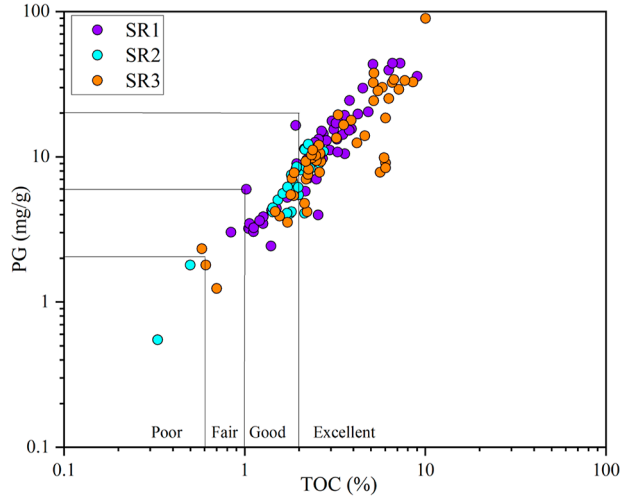

Figure 10. Cross plot of TOC vs PG from the shale samples of the SR1, SR2, and SR3 in the Weixinan sag. (Note: PG = S_1 + S_2, S_1 = free hydrocarbons; S_2 = potential hydrocarbons; and TOC = total organic carbon.)

values (2.43−44.11 mg/g, average = 13.9 mg/g). The source rocks from the middle hydrocarbon combination (SR2) have lower hydrocarbon potential with low TOC values (0.33−2.74%, average = 1.92%) and low PG values (0.55−12.23 mg/g, average = 6.96 mg/g). In comparison, the shales from the lower hydrocarbon combination (SR3) are mostly excellent source rocks, and their TOC values range from 0.58 to 10.03% (average = 3.77%).

The T_{max} values of all source rocks range from 372 to 448 °C, showing a difference from low maturity to high maturity. However, because the wells are located in the margin of subsags, their thermal maturity is far less than the source rocks in the center of basin, where the oils were generated from. Based on these data, we assume that the source rocks generating oils are in the mature−high mature stage. Shales from these three hydrocarbon supply combinations mainly contain type III to type I kerogen. Overall, source rocks from the SR3 are greater than those from SR1 and SR2. The shales from the SR2 are in the poorer quality.

The stable carbon isotope of kerogen is widely used to identify the biological OM and the depositional condition of source rocks. The heavy carbon isotopic signature has been a characteristic of shales containing *Botryococcus* and *Pediastrum* algal.[58] In the Weixinan sag, abundant *Botryococcus*, *Pediastrum,* and dinoflagellate cysts were observed in the organic-rich shales from the E_1^2 formation.[55] The lacustrine facies exhibit the largest isotopic variability. The $\delta^{13}C$ of SR1 source rocks range from −29.13‰ to −26.10‰ with an average of −27.83‰. The $\delta^{13}C$ values vary in the SR2 source rocks from −30.14‰ to −26.10‰ (average = −28.14‰), whereas they are the heaviest one in the SR3 source rocks (−27.52‰ − −21.22‰; average = −25.93‰; Table 4). The enrichment of ^{13}C in the SR3 shales implies a flourish of dinoflagellates compared to the SR1 and SR2 source rocks.

4.2.2. Molecular Geochemistry. The distribution diversities in *n*-alkanes and isoprenoids of the SR1 and SR3 source rocks are shown in Figure 11. The *n*-alkane carbon numbers range from C_{10} to C_{40}, with maxima at C_{23}. The TAR ratios range from 0.42 to 2.31 with an average of 1.25. The OEP values in the SR1 are mostly >1 (1.16−1.88, average = 1.43), except for the sample from WZ592 (0.78), indicating a low maturity. However, the relatively low OEP (1.05−1.12, average = 1.08) and CPI (1.07−1.15, average = 1.10) values exhibit that the SR3 shales are more mature than the SR1. The Pr/Ph ratios of shales from the SR1 range from 1.19−3.59 with an average of 2.28, suggesting that the SR1 source rocks were deposited in a

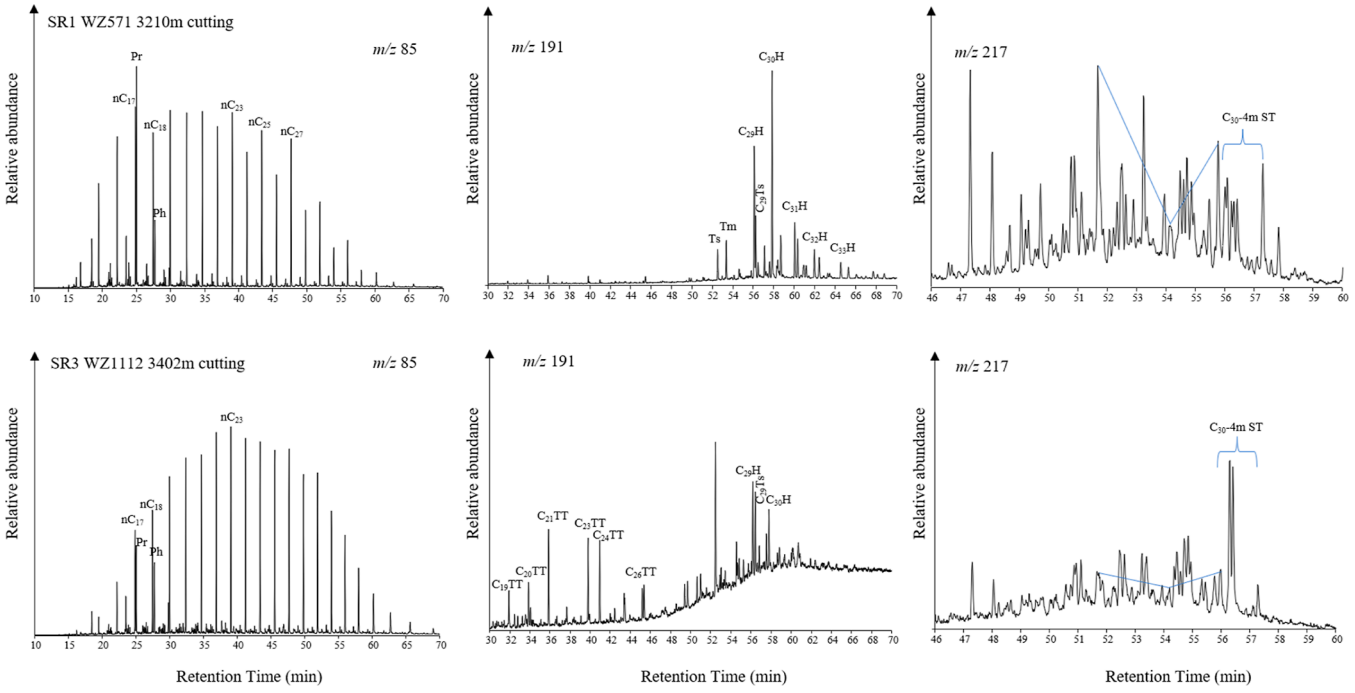

Figure 11. Typical biomarker distributions of shale samples from SR1 and SR3 in the Weixinan sag, showing in the order of *n*-alkane (*m*/*z* 85), terpane (*m*/*z* 191), and sterane (*m*/*z* 217) distribution. (Note: SR1 = the upper hydrocarbon supply combination; SR3 = the lower hydrocarbon supply combination.)

https://doi.org/10.1021/acsomega.2c02826
ACS Omega 2022, 7, 24795−24811

freshwater environment with a dominant higher plant input. In comparison, the ratios of Pr/Ph are in the range of 1.21−1.72 (average = 1.42), showing a weakly oxidized environment during the deposition of SR3 source rocks. It is consistent with gammacerane/C_{30}H (0.004−0.11; average = 0.02; Table 5), which indicates a freshwater environment as well. The oleanane/C_{30}H ratios of source rocks from the SR1 range from 0.01−2.35 (average = 0.25), which is higher than that in SR3 (0.18−0.21; average = 0.19). Ts/(Ts + Tm) ranges from 0.15−0.68 with an average of 0.42 in the SR1, while that of the SR3 is in the range of 0.87−0.96 (average 0.91). This indicates that the thermal maturity of the SR1 is much lower than that of the shales from the SR3, which have been in the high-mature stage. It has a good agreement with other thermal maturity-related parameters (e.g., C_{31} 20R $\alpha\beta$ hopane/C_{30} $\alpha\beta$ hopane, C_{29} $\beta\beta/(\alpha\alpha + \beta\beta)$), indicating the highest maturity in the SR3 source rocks. The distribution of C_{27}−C_{28}−C_{29} $\alpha\alpha\alpha$ 20R sterane mostly exhibits a "L" shape in the SR1 and "V" shape in the SR3 (Figure 11). The 4-MSI in the SR1 ranges from 0 to 0.69 with an average of 0.38, which is much lower than that in the SR3 (1.07−2.52; average = 1.65, Table 5). The studies reported by Boreham et al.[58] and Summons et al.[59] suggested that 4-MSI is related to the bloom of algae, especially dinoflagellates. According to the OM evaluation criteria reported by Fu,[11] the variation of 4-MSI implies that the best source rocks are from SR3, followed by SR1. It also has a good agreement with the results suggested by TOC and PG values.

4.3. Oil−Source Rock Correlation. As outlined above, several source-related parameters, such as oleanane/C_{30}H, C_{19}TT/(C_{19}TT + C_{23}TT), are affected by thermal maturity, so that they are inaccurate to be used as the basis for oil−source rock correlation. However, the $\delta^{13}C_{oil}$, TAR, C_{24}Te/C_{23}TT, ETR, and 4-MSI are not/slightly affected by thermal maturity. Thus, on the basis of these indicators, together with physical properties and thermal maturity-related parameters (e.g., Ts/(Ts + Tm), C_{29}Ts/(C_{29}Ts + C_{29}H), C_{30} diaphone/(C_{30}diahopane + C_{30}H)), three groups of oils were classified. The A1 oil family, occurring in the El^1 reservoir located near the center of sub-sag A, was characterized by high density and low thermal maturity (Ts/(Ts + Tm) < 0.42). Their source rocks were deposited in the freshwater environment with mixed OM and a small input of dinoflagellates. It is supported by the high Pr/Ph values (average 2.22), low ETR (average 0.27) and Ga/C_{30}H (average 0.05), high TAR (average 2.03), and low 4-MSI (average 0.70). The A2 oils, which are distributed in Ew and El^1 reservoirs close to the no. 2 fault, have medium density and moderate thermal maturity. They were derived from the source rocks deposited in a freshwater environment with agal inputs. It is consistent with the medium Pr/Ph values (average 1.45), ETR (average 0.31) and Ga/C_{30}H (average 0.06), low TAR (average 0.73), and medium 4-MSI (average 1.71). The A3 oils, discovered in El^3 reservoirs far from the depression, were distinguished by light density and higher thermal maturity. They were generated from the best source rocks deposited in a subanoxic environment with a large input of algae, especially dinoflagellates.

According to the geochemical characteristics of source rocks, there are three hydrocarbon combinations (SR1, SR2, and SR3). The SR1 shales are good-great source rocks, which are deposited in a freshwater environment with mixed OM (Figure 7a,b). Although there is a lack of the molecular geochemical data of the SR2 source rocks, their carbon isotope of kerogen was compared with those of the SR1 and SR3 to predict the hydrocarbon potential of the source rocks (Table 4). It is suggested that the SR2 are fairly good source rocks with moderate thermal maturity, and their depositional environment is similar to that of the SR1. In comparison, the SR3 source rocks have the greatest hydrocarbon potential, which were formed in a weakly oxidizing environment with the dominated algal input suggested by high abundance of C_{30} 4-methylsterane.

Based on the discussion about these oil families and hydrocarbon supply combinations, coupling with the cross plots (Figures 7a,b, 9 and 12), one supposition on oil−source

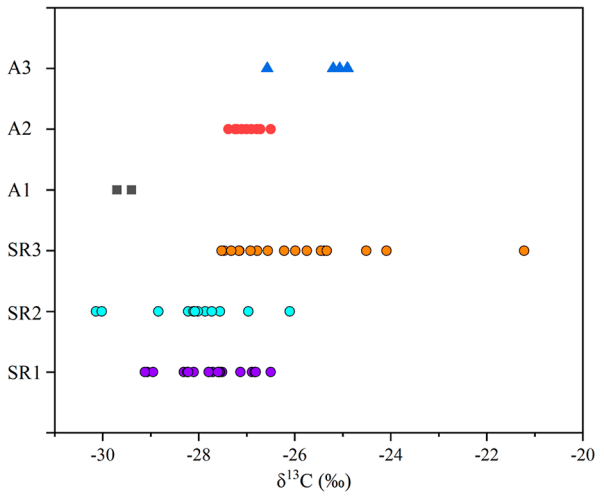

Figure 12. Correlation of three oil families with corresponding kerogens of three source rock combinations based on their $\delta^{13}C$ variations. (Note: SR1 = the upper hydrocarbon supply combination; SR2 = the middle hydrocarbon supply combination; and SR3 = the lower hydrocarbon supply combination.)

relationship in the sub-sag A was that the A1 oils are generated from the SR1 source rocks in the center, the A2 oils are mixed oils from the SR2 and SR3 shales, whereas, the A3 oils were derived from the SR3 shales.

To verify the correctness of the oil−source relationship, the research on the structure of sub-sag A was carried out. According to previous studies, it is found that there are no any faults except the no. 1 fault in the northern of sub-sag A, where the A1 oils are located in. Thus, we proposed that the A1 oils are derived from the SR1 source rocks near the reservoir. The A2 oil family is distributed in the northern of no. 2 fault, and there are many small faults. Therefore, the oils generated from SR2 and SR1 source rocks immigrated along small faults into WZ111 reservoirs. Although the faults in the sub-sag A are not developed, there are two major tectonic ridges: WZ103 and WZ61.[60] Through basin simulations, it is found that oils migrated and accumulated along tectonic ridges. Thus, we proposed that the A3 oils were generated from the SR3 source rocks and migrated along the WZ103 and WZ61 and accumulated in the WZ103 and WZ61 reservoirs.

5. CONCLUSIONS

Three sets of source rocks were identified in the Weixinan sag, including the upper hydrocarbon supply combination (SR1), the middle hydrocarbon supply combination (SR2), and the lower hydrocarbon supply combination (SR3). The SR3 source rocks have the best hydrocarbon potential, which are

https://doi.org/10.1021/acsomega.2c02826
ACS Omega 2022, 7, 24795−24811

in the high-maturity stage. They are characterized by heavy $\delta^{13}C$ values, high 4-MSI, and lower Pr/Ph values, suggesting that they are formed in a freshwater environment with algal bloom. The SR2 source rocks feature middle $\delta^{13}C$ values, which is similar to the SR1 source rocks. They are formed in a freshwater environment with mixed OM, whereas the thermal maturity of the SR2 shales is higher than that of the SR1.

Three oil families (A1, A2, and A3) were classified in the sub-sag A in the Weixinan Depression by a large amount of parameters related to the biological source, depositional environment, and thermal maturity, such as $\delta^{13}C_{oil}$, $\delta^{13}C_{sat}$, $\delta^{13}C_{aro}$, Pr/Ph, 4-MSI, and Ts/(Ts + Tm). The A1 oils are in the low-mature stage, which is originated from the good source rocks deposited in the suboxic environment with terrigenous OM. The A2 oils are in the medium-mature stage, which is derived from the shales' subanoxic environment with mixed OM and an input of dinoflagellates. The A3 oils are in the high-mature stage, which is generated from the great source rocks deposited in a subanoxic environment with the algal bloom.

The oil−source correlation results show that the possible source rocks of the A1 oils are from the SR1, those of the A2 oils are mixed from the SR2 and SR3, and those of the A3 oils are from the SR3.

AUTHOR INFORMATION

Corresponding Authors

Lin Wei − *School of Energy Resources and Key Laboratory of Marine Reservoir Evolution and Hydrocarbon Accumulation Mechanism, Ministry of Education, China University of Geosciences, Beijing 100083, China; Beijing Key Laboratory of Unconventional Natural Gas Geological Evaluation and Development Engineering, Beijing 100083, China;* orcid.org/0000-0002-6243-1581; Email: linwei@cugb.edu.cn

Dujie Hou − *School of Energy Resources and Key Laboratory of Marine Reservoir Evolution and Hydrocarbon Accumulation Mechanism, Ministry of Education, China University of Geosciences, Beijing 100083, China; Beijing Key Laboratory of Unconventional Natural Gas Geological Evaluation and Development Engineering, Beijing 100083, China;* orcid.org/0000-0003-2001-4082; Email: houdj313@163.com

Authors

Xiaoxiao Ma − *School of Energy Resources and Key Laboratory of Marine Reservoir Evolution and Hydrocarbon Accumulation Mechanism, Ministry of Education, China University of Geosciences, Beijing 100083, China; Beijing Key Laboratory of Unconventional Natural Gas Geological Evaluation and Development Engineering, Beijing 100083, China*

Changgui Xu − *Zhanjiang Branch of China National Offshore Oil Corporation Ltd., Zhanjiang 524057, China*

Yong Man − *Zhanjiang Branch of China National Offshore Oil Corporation Ltd., Zhanjiang 524057, China*

Wenlong Li − *Zhanjiang Branch of China National Offshore Oil Corporation Ltd., Zhanjiang 524057, China*

Piao Wu − *Qingdao Institute of Marine Geology, Qingdao 266237, China*

Complete contact information is available at: https://pubs.acs.org/10.1021/acsomega.2c02826

Notes

The authors declare no competing financial interest.

ACKNOWLEDGMENTS

The work was financially supported by Key S&T Special Projects of COONC (project no.: CNOOC-KJ 135 ZDXM 38 ZJ). We gratefully acknowledge the Zhanjiang Branch of the China National Offshore Oil Corporation for sample and data collection.

REFERENCES

(1) Fan, R.; Li, S.; He, S.; Wang, X. L.; Hu, S. Z.; Zhang, D. M. Geochemical characteristics of source rocks and oil-source correlation in Weixinan Sag, Beibuwan Basin. *Pet. Geol. Exp.* **2014**, *36*, 238−244.

(2) Hu, W.; Wu, C.; Liang, J.; Hu, F.; Cai, F.; Chai, H.; Zou, Q. Tectonic transport characteristics and their influences on hydrocarbon accumulation in Beibuwan Basin. *Oil Gas Geol.* **2011**, *32*, 920−927.

(3) Zhang, Z.; Zhan, W.; Tang, M.; Zhou, P.; Wang, W. Subsidence of Beibuwan Basin since Late Miocene. *Mar. Geol. Quat. Geol.* **2013**, *33*, 9−13.

(4) Huang, B.; Xiao, X.; Cai, D.; Wilkins, R. W. T.; Liu, M. Oil families and their source rocks in the Weixinan Sub-basin, Beibuwan Basin, South China Sea. *Org. Geochem.* **2011**, *42*, 134−145.

(5) Jin, Q. Genesis types and accumulation characteristics of crude oil in southeast slope of Weixinan Depression,Beibuwan Basin. *Lithol. Reservoirs* **2020**, *32*, 11−18.

(6) Wang, Y.-P.; Zhan, X.; Luo, T.; Gao, Y.; Xia, J.; Wang, S.; Zou, Y.-R. Oil chemometrics and geochemical correlation in the Weixinan Sag, Beibuwan Basin, South China Sea. *Energy Explor. Exploit.* **2020**, *38*, 2695−2710.

(7) Liu, E.; Wang, H.; Li, Y.; Zhou, W.; Leonard, N. D.; Lin, Z.; Ma, Q. Sedimentary characteristics and tectonic setting of sublacustrine fans in a half-graben rift depression, Beibuwan Basin, South China Sea. *Mar. Pet. Geol.* **2014**, *52*, 9−21.

(8) Bao, J.; Zhu, C.; Ni, C. Distribution and composition of biomarkers in crude oils from different sags of Beibuwan Basin. *Acta Sedimentol. Sin.* **2007**, *25*, 646−652.

(9) Huang, B.; Huang, H.; Wu, G.; You, J. Geochemical characteristics and formation mechanism of Eocene lacustrine organic-rich shales in the Beibuwan Basin. *Acta Pet. Sin.* **2012**, *33*, 25−31.

(10) Fu, N.; Liu, J. Hydrocarbon generation and accumulation characteristics of three type source rocks of LiuIIsegment in Beibuwan Basin. *Nat. Gas Geosci.* **2018**, *29*, 932−941.

(11) Fu, N. On relationship between abundance of 4-methyl-C_{30} sterane and source rock quality: A case study of exploration practices in Beibuwan basin. *China Offshore Oil Gas* **2018**, *30*, 11−20.

(12) Ding, W.; Hou, D.; Gan, J.; Wu, P.; Zhang, M.; George, S. C. Palaeovegetation variation in response to the late Oligocene-early Miocene East Asian summer monsoon in the Ying-Qiong Basin, South China Sea. *Palaeogeogr., Palaeoclimatol., Palaeoecol.* **2021**, *567*, 110205.

(13) Ding, W.; Hou, D.; Jiang, L.; Jiang, Y.; Wu, P. High abundance of carotanes in the brackish-saline lacustrine sediments: A possible cyanobacteria source? *Int. J. Coal Geol.* **2020**, *219*, 103373.

(14) Cai, C.; Zhang, C.; Worden, R. H.; Wang, T.; Li, H.; Jiang, L.; Huang, S.; Zhang, B. Application of sulfur and carbon isotopes to oil-source rock correlation: A case study from the Tazhong area, Tarim Basin, China. *Org. Geochem.* **2015**, *83-84*, 140−152.

(15) Hou, D.; Feng, Z. *Petroleum Geochemistry*; Petroleum Industry Press: Beijing, 2011; pp 278−302.

(16) Dou, L.; Zhu, Y.; Yang, T.; Xu, S.; Ping, X. Origins of heavy oils in the Erlian Basin, NE China. *Mar. Pet. Geol.* **1998**, *15*, 769−781.

(17) Chung, H. M.; Rooney, M. A.; Toon, M. B.; Claypool, G. E. Carbon isotope composition of marine crude oils. *AAPG Bull.* **1992**, *76*, 1000−1007.

https://doi.org/10.1021/acsomega.2c02826
ACS Omega 2022, 7, 24795−24811

(18) Collister, J. W.; Wavrek, D. A. $\delta^{13}C$ compositions of saturate and aromatic fractions of lacustrine oils and bitumens: evidence for water column stratification. *Org. Geochem.* **1996**, *24*, 913−920.
(19) Albaghdady, A.; Philp, R. P. Organic geochemical characterization of crude oils and source rocks from Concession 6, central Sirt Basin, Libya. *Arabian J. Geosci.* **2020**, *13*, 1−31.
(20) Sofer, Z. Stable carbon isotope compositions of crude oils: Application to source depositional-environments and petroleum alteration. *AAPG Bull.* **1984**, *68*, 31−49.
(21) Sun, Y.; Chen, Z.; Xu, S.; Cai, P. Stable carbon and hydrogen isotopic fractionation of individual n-alkanes accompanying biodegradation: evidence from a group of progressively biodegraded oils. *Org. Geochem.* **2005**, *36*, 225−238.
(22) Marcano, N.; Larter, S.; Mayer, B. The impact of severe biodegradation on the molecular and stable (C, H, N, S) isotopic compositions of oils in the Alberta Basin, Canada. *Org. Geochem.* **2013**, *59*, 114−132.
(23) Sun, Y.; Li, Y.; Huang, Z. Abnormal carbon isotopic compositions in organic matter of lacustrine source rocks close to sea. *Pet. Explor. Dev.* **2009**, *36*, 609−616.
(24) Fu, J.; Zhang, Z.; Chen, C.; Wang, T.-G.; Li, M.; Ali, S.; Lu, X.; Dai, J. Geochemistry and origins of petroleum in the Neogene reservoirs of the Baiyun Sag, Pearl River Mouth Basin. *Mar. Pet. Geol.* **2019**, *107*, 127−141.
(25) Quan, Y.; Liu, J.; Hao, F.; Bao, X.; Xu, S.; Teng, C.; Wang, Z. Geochemical characteristics and origins of natural gas in the Zhu III sub-basin, Pearl River Mouth Basin, China. *Mar. Pet. Geol.* **2019**, *101*, 117−131.
(26) Xu, J.; Mao, S. A new understanding of the Bohaidinioid dinoflagellates. *Acta Bot. Sin.* **1989**, *31*, 300−306.
(27) Cranwell, P. A.; Eglinton, G.; Robinson, N. Lipids of aquatic organisms as potential contributors to lacustrine sediments-II. *Org. Geochem.* **1987**, *11*, 513−527.
(28) dos Santos Neto, E. V.; Hayes, J. M.; Takaki, T. Isotopic biogeochemistry of the Neocomian lacustrine and Upper Aptian marine-evaporitic sediments of the Potiguar Basin, Northeastern Brazil. *Org. Geochem.* **1998**, *28*, 361−381.
(29) Moldowan, J. M.; Seifert, W. K.; Gallegos, E. J. Relationship between petroleum composition and depositional environment of petroleum source rocks. *AAPG Bull.* **1985**, *69*, 1255−1268.
(30) Albrecht, P.; Vandenbroucke, M.; Mandengué, M. Geochemical studies on the organic matter from the Douala Basin (Cameroon)—I. Evolution of the extractable organic matter and the formation of petroleum. *Geochim. Cosmochim. Acta* **1976**, *40*, 791−799.
(31) Vuković, N.; Životić, D.; Mendonça Filho, J. G.; Kravić-Stevović, T.; Hámor-Vidó, M.; Mendonça, J. O.; Stojanović, K. The assessment of maturation changes of humic coal organic matter - Insights from closed-system pyrolysis experiments. *Int. J. Coal Geol.* **2016**, *154−155*, 213−239.
(32) Didyk, B. M.; Simoneit, B. R. T.; Brassell, S. C.; Eglinton, G. Organic geochemical indicators of palaeoenvironmental conditions of sedimentation. *Nature* **1978**, *272*, 216−222.
(33) Bernard, T. P.; Welte, D. H. *Petroleum Formation and Occurrence*; Springer: Berlin, 1984.
(34) Greenwood, P. F.; Arouri, K. R.; George, S. C. Tricyclic terpenoid composition of tasmanites kerogen as determined by pyrolysis GC-MS. *Geochim. Cosmochim. Acta* **2000**, *64*, 1249−1263.
(35) Simoneit, B. R. T.; Grimalt, J. O.; Wang, T. G.; Cox, R. E.; Hatcher, P. G.; Nissenbaum, A. Cyclic terpenoids of contemporary resinous plant detritus and of fossil woods, ambers and coals. *Org. Geochem.* **1986**, *10*, 877−889.
(36) Peters, K. E.; Moldowan, J. M. *The Biomarker Guide: Interpreting Molecular Fossils in Petroleum and Ancient Sediments*; Prentice Hall: Englewood Cliffs, NJ, 1993; p 363.
(37) Zumberge, J. E. Prediction of source rock characteristics based on terpane biomarkers in crude oils: A multivariate statistical approach. *Geochim. Cosmochim. Acta* **1987**, *51*, 1625−1637.
(38) Van Aarssen, B. G. K.; Alexander, R.; Kagi, R. I. Higher plant biomarkers reflect palaeovegetation changes during Jurassic times. *Geochim. Cosmochim. Acta* **2000**, *64*, 1417−1424.
(39) Peters, K. E.; Walters, C. C.; Moldowan, J. M. *The Biomarker Guide, Volume 2: Biomarkers and Isotopes in Petroleum Exploration and Earth History*, 2nd ed.; Cambridge University Press: Cambridge, U.K., 2005; p 679.
(40) Kong, X.; Jiang, Z.; Zheng, Y.; Xiao, M.; Chen, C.; Yuan, H.; Chen, F.; Wu, S.; Zhang, J.; Han, C.; Liu, S. Organic geochemical characteristics and organic matter enrichment of mudstones in an Eocene saline lake, Qianjiang Depression, Hubei Province, China. *Mar. Pet. Geol.* **2020**, *114*, 104194.
(41) He, T.; Lu, S.; Li, W.; Tan, Z.; Zhang, X. Effect of Salinity on Source Rock Formation and Its Control on the Oil Content in Shales in the Hetaoyuan Formation from the Biyang Depression, Nanxiang Basin, Central China. *Energy Fuels* **2018**, *32*, 6698−6707.
(42) Philp, R. P.; Gilbert, T. D. Biomarker distributions in Australian oils Predominantly Derived From Terrigenous Source Material. *Org. Geochem.* **1986**, *10*, 73−84.
(43) Edwards, D. S.; Preston, J. C.; Kennard, J. M.; Boreham, C. J.; van Aarssen, B. G. K.; Summons, R. E.; Zumberge, J. E. Geochemical characteristics of hydrocarbons from the Vulcan Sub-basin, western Bonaparte Basin, Australia. *Timor Sea Pet. Geosci.* **2003**, *1*, 169−201.
(44) Ekweozor, C. M.; Telnaes, N. Oleanane parameter—verification by quantitative study of the biomarker occurrence in sediments of the Niger Delta. *Org. Geochem.* **1990**, *16*, 401−413.
(45) Tyson, R. Book Review: *The Biomarker Guide*. *Geol. Mag.* **2006**, *143*, 249−254.
(46) Sinninghe Damsté, J. S.; Kenig, F.; Koopmans, M. P.; Köster, J.; Schouten, S.; Hayes, J. M.; de Leeuw, J. W. Evidence for gammacerane as an indicator of water column stratification. *Geochim. Cosmochim. Acta* **1995**, *59*, 1895−1900.
(47) Fu, J. M.; Xu, F. F.; Chen, D. Y.; Liu, D. H.; Hu, C. Y.; Jia, R. F.; Xu, S. P.; Brassell, A. S.; Eglinton, G. Biomarker compounds of biological inputs in Maoming Oil-Shale. *Geochimica* **1985**, 99−114.
(48) Goodwin, N. S.; Mann, A. L.; Patience, R. L. Structure and significance of C_{30} 4-methyl steranes in lacustrine shales and oils. *Org. Geochem.* **1988**, *12*, 495−506.
(49) Brassell, S. C.; Sheng, G. Y.; Fu, J. M.; Eglinton, G. Biological markers in lacustrine Chinese oil shales. In *Advances in Organic Geochemistry*; Leythaeuser, D., Rulkotter, J., Eds.; Pergamon Press: Oxford, U.K., 1988; pp 927−941.
(50) Sabel, M.; Bechtel, A.; Püttmann, W.; Hoernes, S. Palaeoenvironment of the Eocene Eckfeld Maar lake (Germany): implications from geochemical analysis of the oil shale sequence. *Org. Geochem.* **2005**, *36*, 873−891.
(51) Huang, B.; Zhu, W.; Tian, H.; Jin, Q.; Xiao, X.; Hu, C. Characterization of Eocene lacustrine source rocks and their oils in the Beibuwan Basin, offshore South China Sea. *AAPG Bull.* **2017**, *101*, 1395−1423.
(52) Li, Y.; Lan, L.; Wang, K.; Yang, Y. Differences in lacustrine source rocks of Liushagang Formation in the Beibuwan Basin. *Acta Pet. Sin.* **2019**, *40*, 1451−1459.
(53) Yu, S.; Deng, Y.; Li, H.; Xiao, L.; Wu, A.; Li, F.; Zhang, Z. Forming conditions and distribution controlling factors of oil shale in Liu 2 Member of Beibuwan basin. *China Offshore Oil Gas* **2020**, *32*, 24−33.
(54) Gan, H.; Wang, H.; Shi, Y.; Ma, Q.; Liu, E.; Yan, D.; Pan, Z. Geochemical characteristics and genetic origin of crude oil in the Fushan, sag, Beibuwan Basin, South China Sea. *Mar. Pet. Geol.* **2020**, *112*, 104114.
(55) Huang, B.; Tian, H.; Wilkins, R. W. T.; Xiao, X.; Li, L. Geochemical characteristics, palaeoenvironment and formation model of Eocene organic-rich shales in the Beibuwan Basin, South China Sea. *Mar. Pet. Geol.* **2013**, *48*, 77−89.
(56) Fu, N.; Lin, Q.; Wang, K. Main source rock reevaluation of Member 2 of Liushagang Formation in the sags of Beibuwan basin. *China Offshore Oil Gas* **2017**, *29*, 12−21.

https://doi.org/10.1021/acsomega.2c02826
ACS Omega 2022, 7, 24795−24811

(57) Xu, X.; Wang, B.; Li, X.; Liu, M.; Zhang, Y.; Huang, B. Oil Sources of Concealed Reservoirs in Liushagang Formation of the Weixinan Sag and Accumulation Feature,Beibuwan Basin. *Nat. Gas Geosci.* **2012**, *23*, 92−98.
(58) Boreham, C. J.; Summons, R. E.; Roksandic, Z.; Dowling, L. M.; Hutton, A. C. Chemical, molecular and isotopic differentiation of organic facies in the Tertiary lacustrine Duaringa oil-shale deposit, Queensland, Australia. *Org. Geochem.* **1994**, *21*, 685−712.
(59) Summons, R. E.; Thomas, J.; Maxwell, J. R.; Boreham, C. J. Secular and environmental constraints on the occurrence of dinosterane in sediments. *Geochim. Cosmochim. Acta* **1992**, *56*, 2437−2444.
(60) Li, S.; Yang, X. Characteristics of hydrocarbon migration and accumulation in Weixinan sag of Beibuwan Basin. *Global Geol.* **2012**, *31*, 365−370.

https://doi.org/10.1021/acsomega.2c02826
ACS Omega 2022, 7, 24795−24811